Carbon Sequestration via Concrete Weathering in Soil

Thesis

Presented in Partial Fulfillment of the Requirements for the Degree Master of Science in the Graduate School of The Ohio State University

By

Brittany Multer

Graduate Program in Environment and Natural Resources

The Ohio State University

2023

Thesis Committee

Dr. Rattan Lal, Advisor

Dr. Berry Lyons

Dr. M. Scott Demyan

Dr. Matt O'Reilly

Abstract

Since the beginning of time Earth's carbon cycle has self-regulated, experiencing periods of warming and cooling with changing amounts of carbon in the atmosphere. Today, human activity is rapidly changing the climate through the addition of greenhouse gases to the atmosphere like carbon dioxide (CO_2). To prevent disastrous outcomes caused by climate change, it is vital to halt greenhouse gas emissions, however, this is only one part of the solution. To keep global temperatures from increasing more than 2° C, CO_2 removal must also be an integral part of the solution. The objectives of this research were to conduct a laboratory experiment and investigate the carbonation of concrete within soil as a viable option to sequester atmospheric carbon, analyze how concrete carbonation changes with fragment size, and understand the environmental impacts of adding concrete to soil.

Soil samples from Waterman Agricultural and Natural Resources Center were collected and placed into 30 cm columns with different mixtures of crushed recycled concrete to test concrete in soil as an enhanced weathering material. Four different treatments were tested and were comprised of 1) 100% soil (S samples), 2) 90% soil and 10% concrete by weight of 0.25-0.71 mm diameter fragments (F samples), 3) 90% soil and 10% concrete by weight of 8 mm diameter fragments (L samples), and 4) 100% concrete composed of 8 mm diameter fragments (C samples). Four replications of each treatment

were tested for a total of 16 samples. Approximately 40 cm^3 of deionized water was added to each sample every day from a drip irrigation system for a total amount of 940-990 mm yr^{-1} throughout the experiment to simulate the amount of precipitation received by Columbus, OH in one year, with leachate continuously collected underneath the columns. After 16 weeks, the soil and concrete mixtures were removed from the columns and tests were conducted on the soil and leachate samples.

The results from this study show that concrete in soil has potential as an enhanced weathering material to sequester large amounts of carbon dioxide from the atmosphere. Significant differences between the C samples and the L and F samples showed that soil facilitates faster concrete weathering rates, and significant differences between the L and F samples showed that the smaller concrete fragments weather faster than larger concrete fragments. This study found that putting 120-150 g of concrete in soil sequestered 0.15-1.8 g of CO_2. Modeling the data, it is predicted that for every 1 m^2 surface area of concrete added to soil, 2.1 g of atmospheric carbon is sequestered annually.

Adding concrete to soil was found to impact soil and water quality. The pH of the L and F leachate samples was not significantly different from S leachate samples, but the soil pH of the F samples was significantly different from the L and S samples. This could make concrete a useful lime substitute or a solution to ocean acidification. Sodium was quickly weathered from concrete both in the presence and absence of soil. Because of the dual release of calcium, soil SAR was not significantly different in the L and F samples compared to the S samples, and concrete could be used as a tool to amend sodic soils. Aggregate stability was not found to be impacted by the addition of concrete. The microbial

community was affected by the presence of concrete, with the fungi, protozoa, and bacteria communities all significantly smaller in the F samples. However, these communities were not impacted in the L samples, proving that concrete can be added to soil without harming microbes. Increased nitrate levels were found in the L and F samples. This increase in leachate nitrate could cause harm to nature and humans by aiding the growth of harmful algal blooms and impacting ground water used as drinking water.

Acknowledgments

I would like to thank my advisor, Dr. Rattan Lal, and my committee members Dr. Berry Lyons, Dr. Scott Demyan, and Dr. Matt O'Reilly for their endless guidance and encouragement. Special thanks to Dr. Sue Welch for her patience and teaching with laboratory testing. Additional thanks to Dr. Ian Howat and the Byrd Polar and Climate Research Center for providing lab space, as well as Kyle Sklenka, Dr. Lisa Burris, Marina Miquilini, Dr. Marília Chiavegato, Dr. Nicola Lorenz, Dave Tomashefski, and Shane Whitacre for their help throughout my experiment. Thanks to The Sustainability Institute at Ohio State and Sigma Xi, The Scientific Research Honor Society, for their financial support of my research. Last but not least, thanks to my friends and family whose support of my ambitions never waivers.

Vita

May 2018 .....B.S. Civil Engineering, University of Kansas

July 2018 - July 2021 .....Civil Engineer, Arup, San Francisco, California

August 2021 – Present .....Graduate Teaching Associate, School of Environment and Natural Resources, The Ohio State University

Field of Study

Major Field: Environment and Natural Resources

Table of Contents

List of Tables

List of Figures

List of Equations

Chapter 1. Introduction

Since the beginning of time Earth's carbon cycle has self-regulated, experiencing periods of warming and cooling as the atmospheric carbon content has changed (Ehleringer et al., 2015). Today, human activity is rapidly changing the climate through the addition of greenhouse gases to the atmosphere (IPCC, 2014). Carbon dioxide (CO_2) is the primary greenhouse gas in the atmosphere fueling climate change (National Academy of Sciences, 2020). This time of dominant human influence, called the Anthropocene, is projected to have catastrophic consequences including more frequent and intense weather events such as extreme rainfall, droughts, cyclones, and wildfires, loss of biodiversity, air pollution, landslides, and sea level rise (IPCC, 2014). To prevent these disastrous outcomes, it is vital to halt greenhouse gas emissions, however, this is only one part of the solution. To keep global temperatures from increasing more than 2°C, CO_2 removal must also be an integral part of the solution (Gasser et al., 2015).

The removal of CO_2 has two pathways: organic and inorganic. Organic carbon removal refers to the removal of CO_2 through living organisms such as photosynthesis. Some organic carbon removal techniques currently employed include reforestation, carbon captured by ocean and coastal ecosystems known as blue carbon habitat restoration, and increasing soil organic carbon with the addition of organic material (Williamson, 2016). Inorganic carbon removal refers to the removal of CO_2 through non-living pathways such

as rock weathering. Historically, CO_2 has been removed from the atmosphere primarily through the chemical weathering of calcium (Ca) or magnesium (Mg) silicate rocks (Berner, 1993). The largest store of carbon is found in the lithosphere in carbonate sedimentary rocks and organic compounds, with sedimentary rock being a CO_2 sink four times greater than organic sediments (Carlson et al., 2001). Inorganic carbon is more stable than organic carbon, existing on a timescale of millions of years (Berner, 1993; Carlson et al., 2001) compared to a timescale of 10s to 1000s of years for soil organic carbon (Holmén, 1992).

Because it takes millions of years for chemical weathering to affect the atmospheric CO_2 concentration, scientists have begun exploring artificially increasing chemical weathering, termed enhanced weathering, as a potential method to combat climate change. Natural rocks such as olivine and wollastonite have been investigated as potential enhanced weathering materials, but studies have shown that the emissions associated with mining and transporting rocks offset much of the carbon captured (Hangx and Spiers, 2009; Renforth et al., 2012). Concrete, the most used synthetic material on Earth (Biernacki et al., 2017), is a prime candidate for enhanced weathering because it is ubiquitous. The weathering of concrete is called concrete carbonation. Made of cement, aggregates, and water, concrete is a widely available alkaline material in the preferred form of calcium oxide (Lackner, 2002), and has the potential to become a vital material in the fight against climate change. Alkaline materials are fit for enhanced weathering because they create high pH solutions to dissolve CO_2 and store carbon as carbonate minerals or dissolved bicarbonate ions (Renforth, 2019). Alkaline materials from manufacturing and the

combustion of coal or biomass, which includes concrete, may be able to store 2.9-8.5 billion tonnes (Pg) of CO_2 annually by 2100 (Renforth, 2019).

The objectives of this research were to conduct a laboratory experiment and investigate the carbonation of concrete within soil as a viable option to sequester atmospheric carbon, analyze how the carbonation of concrete changes with fragment size, and understand the environmental impacts of adding concrete to soil. It was hypothesized that concrete in soil would experience carbonation faster than concrete alone. It was also hypothesized that soil samples with smaller concrete fragments would experience carbonation at a faster rate compared to the larger fragments because of the increased reactivity from increased surface area.

Chapter 2. Literature Review

Geologic weathering and the carbon cycle

The current climate crisis is fueled by excess carbon dioxide (CO_2) in the atmosphere (National Academy of Sciences, 2020). Prior to the Anthropocene, Earth's natural processes balanced the carbon cycle with the main sink of CO_2 in the long-term carbon cycle being chemical weathering (Berner, 1993). Chemical weathering is the breakdown of rocks through a change in chemical composition like hydration, dissolution, or hydrolysis/ion exchange (Gibson and Byerly, 2018). Without chemical weathering as a CO_2 sink, Earth's surface temperature would be closer to 450°C with an atmosphere similar to Venus (Schuiling, 2013). Climate significantly affects the rate of chemical weathering with hot, humid conditions increasing weathering rates (Schuiling, 2013). One type of chemical weathering, called carbonation, occurs when CO_2 from the atmosphere combines with rainwater to form carbonic acid (H_2CO_3) which dissolves part of silicate minerals (Schuiling, 2013). Calcium (Ca) and magnesium (Mg) silicate rocks form secondary clay minerals as end products during carbonation, effectively capturing CO_2 in new minerals (Schuiling, 2013). These new minerals are pedogenic carbonates, or secondary carbonates, which are "carbonates formed and redistributed in soils via dissolution of the SIC pool (i.e., geogenic, biogenic or previously formed pedogenic carbonates) and re-precipitation of dissolved ions in various morphologies such as carbonate nodules" (Zamanian et al., 2016).

Calcium carbonate (calcite; $CaCO_3$) makes up approximately 4% of the Earth's crust by weight (Gibson and Byerly, 2018). It is the main component in limestone and is more likely to form carbonates compared to Mg because it has a larger ionic radius (Gibson and Byerly, 2018). Calcite weathering can be a sink of CO_2; the chemical equation showing the chemical weathering of calcite is shown in Equation 1.

Equation 1 Weathering of calcite

$$CaCO_3 + H_2CO_3 \leftrightarrows Ca^{2+} + 2HCO_3^-$$

Scientists have explored enhanced weathering, or the process of accelerating natural weathering, as a tool to combat climate change because of its ability to drawdown CO_2. The goal of enhanced weathering is to sequester atmospheric CO_2 through the dissolution of silicates to convert CO_2 to bicarbonate in solution (Schuiling, 2013). Schlesinger (1982) noted the importance of examining the net storage of carbon fixation from pedogenic carbonates regarding the calcium source; calcite reprecipitated from calcareous parent material would have little carbon fixation compared to noncalcareous areas with calcium rich parent material. Potential naturally occurring materials that are good candidates for enhanced weathering include olivine basalts, basaltic tuffs, and anorthosites because of their increased weathering rates and availability (Schuiling, 2013). Renforth et al. (2015) investigated the dissolution of olivine in soil. 100 g of crushed and ground olivine was added to soil columns and a nutrient solution was dripped onto the columns over 5 months. The leachate was collected and analyzed for silica (Si), Mg, Ca,

aluminum (Al), chromium (Cr), and iron (Fe) as indicators of dissolution. The study concluded the olivine dissolution rates were approximately 200 Mg km^{-2} a^{-1} which was noted as significantly slower than olivine dissolution rates predicted from laboratory kinetics. The experiment showed olivine to be an effective material for enhanced weathering, however the experiment is not scalable if olivine were to be land applied because of the difficulty and costs associated with widely applying the nutrient solution. Schuiling and Krijgsman (2006) considered the land application of olivine in areas that receive acid rain and noted that olivine is a cheap and widely available material that has potential to improve the quality of forest soil. ten Berge et al. (2012) investigated olivine for enhanced weathering, but also assessed the impacts to plant growth and nutrient uptake. The 32-week experiment applied different amounts of olivine to a pot experiment and found that at all olivine amounts increased plant growth and at the largest dose increased plant potassium (K) concentration. The bioavailability of Mg and nickel (Ni) increased with olivine as well as plant uptake of Mg, Si, and Ni while the uptake of Ca was suppressed. Carbonation observed was lower than predicted, similar to Renforth et al. (2015), which the study concluded to be caused by negative feedback from the soil. CO_2 gross sequestration was calculated to be 290-2690 kg ha^{-1}. Olivine weathering releases elements such as Si, P, and K into solution which can be nutrients for flora and fauna, but airborne rock dust may also be released into the environment which can cause health risks to humans and animals (Hartmann et al., 2013).

Wollastonite is another mineral investigated as a contender for enhanced weathering. A study by Haque et al. (2020) found that wollastonite increased soybean

yields and alfalfa growth and sequestered CO_2 at a rate of 0.08 kg CO_2 m^{-2} mos^{-1}. Manning et al. (2013) looked at the accumulation of inorganic carbon in artificial soils comprised of blended compost with dolerite and basalt quarry fines and found an accumulation rate of carbonate minerals of 4.8 Mg C ha^{-1} a^{-1} with 40% of the carbon being derived from photosynthesis. Kantzas et al. (2022) created a carbon budget model and estimated that enhanced rock weathering of silicate rocks amended to soils across UK arable croplands could remove 6–30 Tg CO_2 a^{-1} by 2050. The study modeled scenarios with different rock particle sizes to reduce milling energy demands and noted that enhanced weathering would decrease nitrous oxide emissions, reverse soil acidification, and reduce fertilizer usage.

Despite the promising results of these studies, the emissions associated with mining and transporting the rocks offset much of the carbon captured. This was shown by Hangx and Spiers (2009) who studied the spreading of olivine along Earth's coastlines as a method to sequester CO_2 but found that the preparation and movement of the material would pose major economic, infrastructure, and public health questions. In the UK, Renforth (2012) presented a case study of enhanced silicate rock weathering that reached the same conclusion. They estimated that that crushing of rocks and transport account for 77-97% of the energy requirements. They concluded there is not enough known on the weathering rates and environmental impact of silicate mineral land application to move forward with this scheme.

Kelemen et al. (2011) noted the costs associated with enhanced weathering of natural rock and proposed enhanced in situ carbonation as an alternative for CO_2 capture. This method involves transporting CO_2 rich fluid to areas with large volumes of olivine.

Further research on this method is required to determine if this is a viable carbon capture technique.

Mining and other processes results in waste products which have potential for enhanced weathering. Magnesium-rich mine tailings formed carbonate crusts from an asbestos mine in New South Wales, Australia with calculated carbonation rates ranging from 27 g C m^{-2} a^{-1} to 1330 g C m^{-2} a^{-1} (Oskierski et al., 2013). The health risks from these tailings are unknown, so more research is needed before these could be utilized for enhanced weathering. Langer et al. (2009) suggested disposing of limestone fines produced from fossil-fuel fired power plants and other point sources into the ocean. Environmental concerns as well as the current abandonment of fossil fuel powered plants make this an unappealing option.

A study by Thornbush and Viles (2007) used a climate chamber to simulate the dissolution of limestone under different carbonic acid concentrations to account for future increased atmospheric CO_2 levels caused by climate change. The simulation found that increased atmospheric CO_2 would accelerate dissolution rates. The increase was partial to newly replaced limestone building stones and previously weathered surfaces were less susceptible to increased rainfall acidity. However, future dissolution rates are not expected to increase enough to mitigate climate change impacts from atmospheric CO_2.

Concrete and carbonation

In its simplest form, concrete is composed of cement, water, and aggregates. Because of the seemingly unlimited uses of concrete, cement is the most used synthetic

material on Earth (Biernacki et al., 2017). Raw materials in Portland cement, the most commonly used cement, include a source of lime (CaO), silica, alumina, and iron oxide (Mamlouk and Zaniewski, 2016). These materials are put into a kiln and heated to extremely high temperatures where cement clinker is formed. When raw materials are heated in the kiln, the reaction shown in Equation 2 occurs.

Equation 2 Creation of CaO from limestone

$$CaCO_3 + heat \rightarrow CaO + CO_2$$

This reaction and the heat required to induce this reaction are responsible for as much as 8% of global CO_2 emissions (Andrew, 2018; Beerling et al., 2020). Table 1 shows the compounds contained in Portland cement.

Table 1 Portland cement compounds

Compound	Chemical composition	% by weight in typical Portland cement*
Tricalcium silicate	$3CaO.SiO_2$	55
Dicalcium silicate	$2CaO.SiO_2$	18
Tricalcium aluminate	$3CaO.Al_2O_3$	10
Tetracalcium aluminoferrite	$4CaO.Al_2O_3Fe_2O_3$	8
Calcium sulfate dihydrate	$CaSO_4.H_2O$	6
Magnesium oxide	MgO	2.6
Sodium oxide	Na_2O	0.3
Potassium oxide	K_2O	0.6

Other	TiO_2; MnO_2	Trace amounts

* Mindess et al., 2003

In addition to the silicates produced during clinkering, gypsum ($CaSO_4.H_2O$) is often added to the final cement product in order to slow the rate of aluminate hydration (Mamlouk and Zaniewski, 2016). Water and cement react into hardened cement paste products during concrete mixing. This reaction, called hydration, forms new compounds; the composition of cement paste is given in Table 2. In addition to water and cement, concrete typically contains coarse and fine aggregate as a filler material. Aggregate materials can vary depending on the region. In 2021, the United States produced 1.5 billion tonnes (Pg) of crushed stone, with 72% of the crushed stone being used as a construction aggregate; 70% of this crushed stone was limestone and dolomite (U.S. Geological Survey, 2022).

Table 2 Cement Paste Compounds

Compound	Chemical formula	% of cement paste*
Calcium hydroxide (Portlandite)	$Ca(OH)_2$	25
Calcium silicate hydrates (C-S-H)	$CaO\text{-}SiO_2\text{-}H_2O$**	60
Calcium sulfoaluminate (Ettringite)	$3CaO.Al_2O_3.{}_3CaSO_4.32H_2O$	15

* Saleh and Eskander, 2020

**Written C-S-H because it has no fixed composition. Typically, twice as much CaO as SiO_2

Changes to the production of concrete have been implemented to lower the carbon footprint. One approach is to replace a fraction of cement with a supplementary cementitious material (SCM). The most common SCMs include fly ash, slag cement, silica fume, and metakaolin (Panesar, 2019). SCMs can reduce the quantity of cement a concrete mix requires which reduces the total carbon footprint, but the inclusion of SCMs can alter concrete physical properties. This may require additives or other adjustments to maintain desired characteristics. SCM replacement of cement is not normally more than 50%, and most SCMs still contain CaO (Panesar, 2019). The typical percent range of CaO in common SCMs is shown in Figure 1.

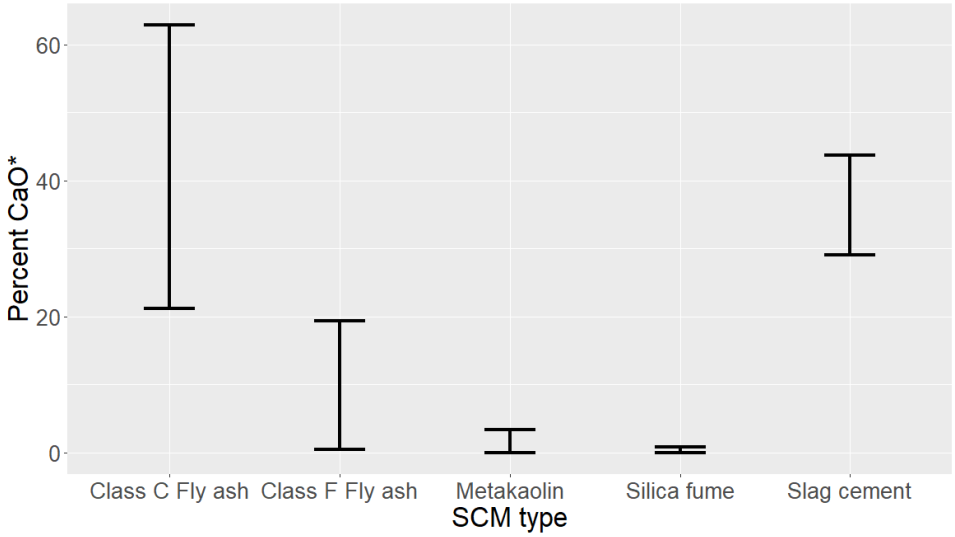

Figure 1 SCM CaO Composition
*Panesar (2019)

The chemical weathering of concrete, known as concrete carbonation, occurs when CO_2 chemically reacts with compounds in concrete to create $CaCO_3$ minerals (Lee and Wang, 2016). Concrete carbonation, mainly of interest to the engineering field, has been

researched because of its impact on concrete properties. Carbonation occurs more with high surface area, relative humidity 50-70%, and a slightly positive pressure (Bertos Fernández et al., 2004). Hydrated cement constituents in Table 2 react following Equation 3, Equation 4, and Equation 5.

Equation 3 Dissolution of Portlandite

$$Ca(OH)_2 + H_2CO_3 \rightarrow CaCO_3 + H_2O$$

Equation 4 Dissolution of C-S-H

(a) $(3CaO \cdot 2SiO_2 \cdot 3H_2O) + 3H_2CO_3 \rightarrow 3CaCO_3 \cdot 2SiO_2 \cdot 3H_2O + 3H_2O$

(b) $(2CaO \cdot SiO_2) + 2H_2CO_3 \rightarrow 2CaCO_3 + SiO_2 \cdot 2H_2O$

(c) $(3CaO \cdot SiO_2) + 3H_2CO_3 \rightarrow 3CaCO_3 + SiO_2 \cdot 3H_2O$

Equation 5 Dissolution of Ettringite

$$(3CaO \cdot Al_2O_3 \cdot 3CaSO_4 \cdot 32H_2O) + 3H_2CO_3 \rightarrow 3CaCO_3 + Al_2O_3 \cdot xH_2O + 3CaSO_4 \cdot 2H_2O + xH_2O$$

Carbonation impacts concrete physical and chemical properties. Carbonation is known to cause corrosion (Cheng et al., 2016). Typical Portland cement concrete has a pH between 12.5 and 13 (Deschner et al., 2012 as cited in Behnood et al., 2016) while natural rainwater has a pH of 5.6 (Charlson and Rodhe, 1982). Carbonation in turn lowers the pH of concrete. This leads to a breakdown of the passive layer around steel rebar reinforcement which causes corrosion and reduces reinforced concrete service life (Chitte and Narkhede,

2016). Porosity, hardness, and hydrological properties of concrete are also affected by carbonation (Choi et al., 2016). Carbonation has been found to increase concrete strength (Shao et al., 2006; Kamal et al., 2020), but it can cause shrinkage and cracking in reinforced concrete products (Shao and Lin, 2011). Carbonation also adversely affects the diffusion resistance of concrete, with adverse effects being more pronounced in cements containing SCMs (Ngala and Page, 1997). Images from Confocal Raman Microscopy show that carbonation is a complex mechanism with cement particles only partially weathering and carbon particles coexisting with amorphous carbon (Torres-Carrasco et al., 2017).

Because of the negative impacts to concrete properties, studies have been undertaken to understand the factors which increase the depth and frequency of carbonation. The depth of carbonation has been found to significantly increase with increasing steel slag replacement of cement (Jiang et al., 2018). The risk of carbonation was also found to increase with elevation and distance from seashore due to marine breezes and humidity (Castro et al., 2000). Longer curing times can improve carbonation resistance, and compressive strength and cement type at initial exposure to carbonation are vital (Ekolu, 2016). Concrete containing SCMs are more vulnerable to carbonation (Panesar, 2019). The inclusion of reinforcing fibers in concrete has been shown to give concrete a slightly increased resistance to carbonation (Ortega-López et al., 2018). Carbonation curing has been shown to reduce corrosion risk due to the formation of a carbonate-rich surface layer (Zhang and Shao, 2016). Carbonation has been found to increase over time with the rate of CO_2 uptake being rapid in the initial stages and slowing

with time (Dayaram et al., 2008). Concrete with higher water to cement (w/c) ratios have been found to absorb more CO_2 (Galan et al., 2010).

A study by Andrade and Sanjuán (2021) investigated carbonation of 15 Portland cement composites with differing cement types and w/cm ratios under different conditions. Specimens placed outdoors were found to uptake up to 30% CO_2 g^{-1} of calcinated cement compared to indoors which took up less than 20%. Relative humidity lower than 40% led to higher uptake in concrete with low w/c ratios while relative humidity greater than 60% led to higher uptake in concrete with high w/c ratios. Ben Ghacham et al. (2015) investigated using waste concrete to sequester CO_2 by direct mineral carbonation, however using this method for larger quantities would be expensive and energy intensive. Inducing carbonation during the concrete mixing process to purposefully incorporate $CaCO_3$ into concrete has been used as a method to reduce the carbon footprint of concrete. However, a study by Ravikumar et al. (2021) found that it was more likely this process had negative CO_2 impacts because of the emissions from transport and the processes to make the concrete, as well as the change in compressive strength and uncertainty and variability in the production process.

Concrete carbonation can also impact water chemistry. One study found that average major ion concentrations in urban watersheds were 25 times higher than forested watersheds due to interactions with weathered impervious surfaces (Moore et al., 2017). Another study performed weathering experiments in the laboratory by introducing 100 mL (cm^3) of water to a small piece of concrete and found increases in concentrations of dissolved inorganic carbon, Ca^{2+}, Mg^{2+}, Na^+, sulfate (SO_4^{2-}), and Si as well as pH (Kaushal

et al., 2017). Similar experiments exposing concrete to rain also note the increased presence of Ca and Si as well as chromium (VI) in simulated runoff (Demars and Benoit, 2019). This has large implications for soil and water quality.

Enhanced weathering of concrete as a tool to sequester carbon

Enhanced weathering has the capability to sequester CO_2, but the emissions associated with mining and transporting natural rocks would offset much if not all of the captured CO_2. This is emphasized by Dunsmore (1992) who concluded that the only source of Ca or Mg which could be extracted at a cost and scale to offset fossil fuels are subsurface brines. Conversely, discarded concrete is readily available around the globe. Concrete carbonation is undesirable during the service life of a structure, but using waste concrete as an enhanced weathering material has immense potential as a carbon sink and would divert millions of tons of concrete waste from landfills. Huang et al. (2020) predicted that concrete construction and demolition waste will reach 7,750 million tonnes (Tg) in 2050 which is three to four times the waste amount in 2000.

Numerous studies have attempted to quantify the carbon capture from concrete carbonation with models. One study showed that for a structure with slag blended concrete, 4.61% of CO_2 would be absorbed for each unit of CO_2 produced during a 50-year service life (Lee and Wang, 2016). Other models predict past CO_2 uptake which offset CO_2 emitted from the decomposition of limestone during cement production, with calculated rates of 55% (Guo et al., 2021), 18-21% (Yang et al., 2014), and 43% (Xi et al., 2016). One case study looked at carbon balances of concrete structures built and demolished from 2018-

2050 and found potential uptake from crushed concrete carbonation over 9% of concrete manufacturing emissions (Ruschi Mendes Saade et al., 2022). Renforth et al. (2011) estimated construction waste has a carbon capture potential of 9−37 Tg C a^{-1} and demolition waste has a carbon capture potential of 24−100 Tg C a^{-1}. Leaching calcium from waste concrete with hydrochloric acid to precipitate $CaCO_3$ via aqueous reaction with sodium carbonate is another possible method with potential but presents difficulty in scaling (Vanderzee et al., 2018). All of these studies emphasize concrete's capacity for carbon sequestration.

Soil organic matter has been widely discussed as a way to sequester carbon, but carbon is stored as carbonates (inorganic carbon) in 80% of instances versus removed through photosynthesis and captured as organic carbon which is done the other 20% of the time (Dunsmore, 1992). As a calcium silicate material, concrete is a prime candidate for enhanced weathering, and using soil as a medium could increase weathering rates. Many processes in soil, including biological, chemical and physical, accelerate mineral weathering, such as macrofauna activity, root exudation, and respiration (Manning and Renforth, 2013). Studies have experimented with the carbonation potential of concrete, but none have done so using soil as a medium in a controlled laboratory experiment. Limestone, the primary raw material for cement, is already commonly applied to agricultural fields as an amendment to neutralize soil acidity (Conyers et al., 2003; Oates, 2010). Liming alternatives such as coal-burning by-products have been explored and have been found to increase soil pH without negatively impacting soil quality (Stehouwer et al., 1995; Stehouwer et al., 1999). A study by Abbaspour and Tanyu (2020) looked at the direct

and indirect carbonation of rubblized concrete over one year. The experiment included "pretreated" particles which were 75μm or less in diameter and "untreated" particles which were 4.75 mm or less in diameter. Direct carbonation was tested by spreading the material in a room with controlled humidity and temperature and exposing it to wetting and drying. Indirect carbonation was tested in two ways. The first used concrete columns exposed to water and the second was with a solution created by shaking concrete in deionized water and creating a brine. The study found that direct carbonation of pretreated rubblized concrete absorbed up to 56 mg g^{-1} of CO_2 and 19 mg g^{-1} of CO_2 when untreated in one year. Possan et al. (2017) looked at the CO_2 uptake of the Itaipu Dam in South American due to concrete carbonation by taking 155 cores from the dam in various locations. The study found that the dam had absorbed over 13,000 tons of CO_2 throughout its service life from concrete carbonation, and that carbonation increases with dam elevation. Concrete carbonation has also been explored in seawater in tandem with alga culture (Takano and Matsunaga, 1995). An experiment by Renforth and Manning (2011) exposing hydrated cement gels to citrate anions, which is a proxy for root exudates in soil, found 80-85% of Ca was leached after 5 hours.

Brownfields containing demolition waste have been studied to understand concrete carbonation in soil. Jorat et al. (2020) looked at concrete carbonation in brownfield sites and found a removal rate of 4-59 Mg CO_2 ha^{-1} a^{-1} with rates being highest in the first 15 years. A study by Washbourne et al. (2012) sampled average carbonate contents at brownfield sites and calculated a CO_2 storage potential of 64,800 Mg CO_2. Another study of urban soils found carbonation extending to a depth of over 1 m and calcium carbonate

contents corresponding to sequestration rates of 85 Mg CO_2 ha^{-1} a^{-1} (Washbourne et al., 2015). Renforth et al. (2009) studied soils containing calcium rich anthropogenic materials, such as demolition waste, and found calcium carbonate storage three times that of expected organic carbon content which accumulated at a rate of 25 ± 12.8 Mg C ha^{-1} a^{-1}. Table 3 shows concrete CO_2 sequestration rates found by existing studies.

Table 3 Concrete Carbonation CO_2 Sequestration Rates

Source	CO_2 sequestration rate (Mg ha^{-1} a^{-1})
Jorat et al., 2020	4-59
Washbourne et al., 2015	85
Renforth et al., 2009	12.8

The impact of concrete carbonation on soil has not been widely monitored, but the studies that have measured soil properties have not found concerning negative effects. Jacques et al. (2010) simulated the chemical degradation of concrete in soil and identified major factors influencing the reaction rates as dry deposition and biological activity because they increase the partial pressure of CO_2. Increased carbonation was found to increase soil bearing capacity but not reduce permeability (Jorat et al., 2020). More data on the influence of concrete carbonation on soil properties is needed.

Chapter 3: Materials and Methods

Sampling

Soil samples were collected from Waterman Agricultural and Natural Resources Center near The Ohio State University Columbus campus on June 28, 2022. Samples were collected from undisturbed grass-covered Miamian silt clay loam soil, per NRCS soil survey maps, at 40.017485° N, -83.040458° W. Soil samples were taken with a soil core sampler (AMS Inc., Idaho, United States) and two stacked cores both 7.6 cm in height and diameter using the core method (Blake and Hartge, 1986). The empty soil cores were weighed before sampling. Samples were wrapped in plastic film to maintain moisture. 16 total soil cores were taken: 12 for experiment samples and 4 for initial soil parameter testing (herein referred to as 'initial soil samples'). Immediately following sampling, bulk density and moisture content were measured for the 4 initial samples. Soil moisture content was calculated by weighing a soil sample before and after being oven dried for 24 hours at 105°C (Gardner, 1986). Bulk density and moisture content were calculated using Equation 6 and Equation 7.

Equation 6 Bulk Density

$$\rho_b = \frac{M}{V} * \frac{1}{(1+w)}$$

ρ_b = bulk density (g/cm^3)

M = mass of wet soil (g)

V = volume of soil core (cm^3)

w = gravimetric water content (g/g)

Equation 7 Gravimetric Moisture Content

$$w = M_w/M_s$$

w = gravimetric water content (g/g)

M_w = mass of water (g)

M_s = mass of soil (g)

Soil samples from each of the four initial soil samples were frozen and sent off for microbial testing. X-ray diffraction (XRD) was completed on two of the initial soil samples with an X'Pert PRO (Malvern Panalytical, Malvern, United Kingdom) to determine soil minerology. An automated particle size analyzer (Meter, Washington, United States) was used to measure particle size distribution using the hydrometer method (Sheldrick and Wang, 1993).

Figure 2 Soil core sampling

Four different treatments were tested and were comprised of 1) 100% soil (S samples), 2) 90% soil and 10% concrete by weight of 0.25-0.71 mm diameter fragments (F samples), 3) 90% soil and 10% concrete by weight of 8 mm diameter fragments (L samples), and 4) 100% concrete composed of 8 mm diameter fragments (C samples). Four replications of each treatment were tested for a total of 16 samples. Concrete used in the experiment was crushed recycled concrete made by the Civil Engineering Department at The Ohio State University in spring of 2022 and was composed of cement, quartz fine aggregate, limestone coarse aggregate, water, superplasticizer, and air. The breakdown of materials by weight per the concrete mix design is shown in Table 4. The superplasticizer used was Sika viscocrete 2100. The concrete was received as a block and was mechanically broken down and sieved to get desired fragment sizes. The experiment was housed in a laboratory in Byrd Polar and Climate Research Center at The Ohio State University Columbus Campus and was kept at 20°C.

Table 4 Concrete components to yield 0.023 m^3 of concrete

Component	kg
Cement	8.74
Water	4.37
Coarse aggregate	21.60
Fine aggregate	15.80
superplasticizer	0.016

Soil column stands were constructed from lumber and used to hold the soil columns. Soil columns were composed of 30 cm long 7.5 cm diameter clear PVC schedule 40 pipe, with a 7.5 cm diameter fitted end cap on the bottom and 0.43 cm diameter clear PVC vinyl tubing leading from the end cap into a collection cup. Filter paper was placed in the bottom of the columns in the end cap to prevent blockage of the tubing. 10 cm^3 syringes were embedded into the top 5 cm of the samples in order to take air samples. An automatic drip irrigation system (Moistenland, Shenzhen, China) was built across the tops of the soil columns to deliver deionized water (DI) from a reservoir to the samples. The reservoir was a Nalgene jug that was refilled as needed. Images from Figure 3 show the laboratory setup. The irrigation system was tested prior to the start of the experiment to determine flow rates to each sample; the irrigation system was determined to have a flow rate of approximately 25 mL/min per sample. The quantity of water added to the samples over the 16-week experiment was equivalent to one calendar years' worth of precipitation for Columbus, Ohio in order to simulate the weathering that would occur in one year. Franklin County, Ohio historically receives 940-990 mm yr^{-1} of precipitation (ODNR, 2011). Using the drip irrigation flow rate and annual precipitation, the drip irrigation system was set to run daily for 90 seconds to deliver ~40 cm^3 day^{-1} to each sample. Samples were watered daily in order to maintain consistency in testing periods. Rainfall typically has a pH of 5.6 (US EPA, 2016). To more closely imitate rainwater chemistry, deionized water was collected in a separate Nalgene jug and left open to the air for at least 24 hours before being added to the reservoir.

Figure 3 Laboratory setup showing the soil column (left), irrigation system (center), and syringe used for air testing (right)

Soil-only samples were placed into the soil columns intact from the soil cores. These samples were labeled S1, S2, S3, and S4. 1000 g of 8 mm diameter concrete fragments was placed into each soil column for the concrete-only samples and labeled C1, C2, C3, and C4. To make the mixed samples, calculations were completed to add an amount of concrete which would constitute 10% of the samples' final weight, shown in Equation 8. The concrete and soil were then mixed in a mixing pan and placed into the soil column. Attempts were made to compact the column to the original density, but this proved difficult, and the samples ultimately were less dense than the original soil cores. This process was completed for all eight mixed samples. Four of these samples were mixed with fine concrete fragments, 0.25-0.71 mm in diameter, and labeled F1, F2, F3, and F4. The other four samples were mixed with large concrete fragments 8 mm in diameter, and labeled L1, L2, L3, L4. Table 5 shows a summary of the samples.

Equation 8 Concrete Weight Calculation

$$c = s/0.9 - s$$

s = soil weight (g)

c = concrete weight (g)

Table 5 Sample summary

Samples	Treatment	Treatment name
C1, C2, C3, C4	Concrete only 8 mm diameter fragment size	C
L1, L2, L3, L4	Soil and concrete, 8 mm diameter fragment size	L
F1, F2, F3, F4	Soil and concrete, 0.25-71 mm diameter fragment size	F
S1, S2, S3, S4	Soil only	S

Leachate was collected continuously in plastic cups beneath the columns. Figure 4 shows the irrigation schematic. Every two weeks samples were filtered into 125 cm^3 wide mouth LDPE bottles using 30 mL syringes and 25-mm diameter 0.45-µm polypropylene syringe filters. Filtered samples were kept in the refrigerator. Sample cups were rinsed out every 2 weeks after filtering. The collection cups began to accumulate material, so starting with sample 3 the cups were wiped with paper towels in addition to being rinsed out.

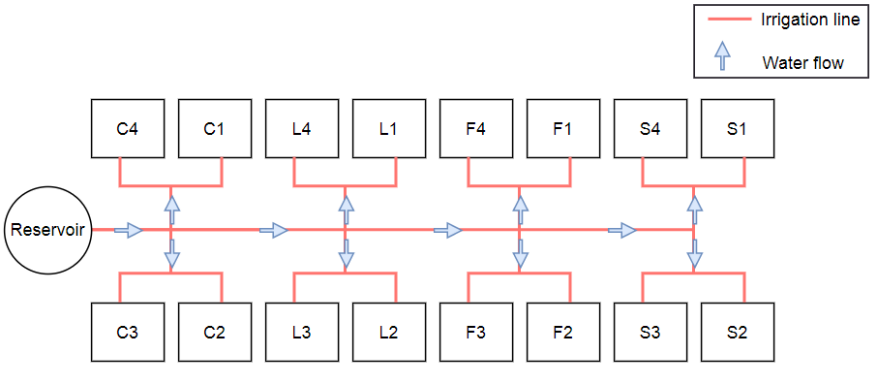

Figure 4 Irrigation Schematic

Air samples were taken every two weeks by placing air sample vials onto the syringes embedded in each sample and letting them collect air for minimum 30 minutes. Samples were tested with a GC-2014 gas chromatograph (GC) (Shimadzu, Kyoto, Japan). Vials were vacuumed after each sample and the lids were replaced after every 2 samples. Samples six through eight were measured with a different gas chromatograph because the previous GC was unable to measure N_2O; because of this change, new vials were used, shown in Figure 5. The GC being used to test samples 6-8 became unavailable as well, so samples remained in the vial for 2-3 months before being analyzed.

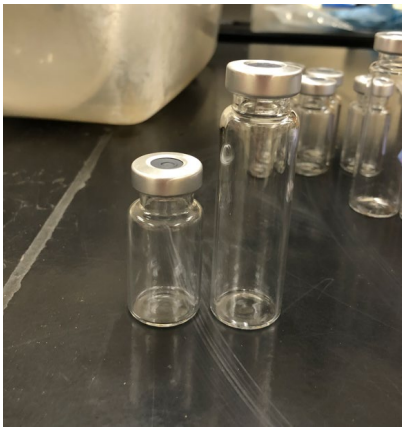

Figure 5 Air sample vials, left for samples 1-5 and right for samples 6-8

Irregularities occurred throughout the experiment. Before sample 3 was collected, it was noticed that the water to samples S1 and S2 was leaking down the column side and bypassing the soil. To correct this, 240 mL of DI water, the amount which the sample should have received during that time, was manually added to the samples. During week 12, sample S4 began having significant amounts of standing water due to a clogged drain. This was unclogged from below by pushing a thin metal conduit through the tubing to dislodge the blockage. Multiple samples had precipitates inside the tubing and in collection cups during the experiment. The tubing for C4 became blocked by a precipitate by the time sample 8 was collected that there was standing water in the column. These precipitates were cleared to permit free water flow.

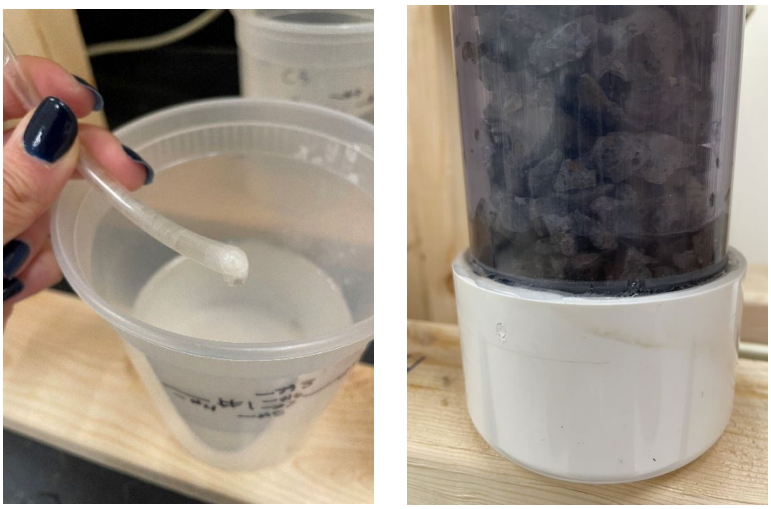

Figure 6 Sample C4-8 mineralization and standing water

After 16 weeks, irrigation of the samples ceased, and final water and air samples were collected. Soil samples from the top 10 cm were collected and frozen for microbial testing. The samples were air dried in the columns for 2 weeks and then removed from the columns and placed into plastic bags to continue air drying.

Testing

Silica, measured as silicon dioxide, and nitrogen, measured as nitrate and nitrite, were analyzed from the leachate using a continuous flow analyzer (Skalar, Netherlands). All samples except C1-C4 were diluted with DI water at a ratio of 0.5:10 cm^3. Major cations and anions were analyzed in the leachate using ion chromatography. A Dionex AS40 autosampler (Thermo Fisher Scientific, Massachusetts, United States) was used for cations and a Dionex AS-DV autosampler (Thermo Fisher Scientific, Massachusetts, United States) was used for anions. All cation samples were diluted with deionized water at a ratio

of 0.5:5 cm^3. A pH meter was used to measure the pH of the leachate (Thermo Fisher Scientific, Massachusetts, United States). pH measurements of the soil samples were taken by mixing 10 mg of <2 mm soil with 20 mL of water, shaking the samples for 30 minutes, and measuring pH and EC with an Aquasearcher AB33EC Bench Meter (OHAUS Corporation, New Jersey, United States). It was observed that the textures of the samples seemed to vary, so a wet sieving aggregate stability test was completed using the Yoder method and a wet sieving apparatus (Yoder, Columbus, Ohio) (Yoder, 1936). Soil microbial testing was done by The Ohio State University Microbial lab using the EL-FAME extraction method (Schutter and Dick, 2000). A 6890N gas chromatograph was used for analysis (Agilent, California, United States). A sodium adsorption ratio test (SAR) was completed using a 700 Series ICP Optical Emission Spectrometer (Agilent, California, United States) to test if the concrete was adding a disproportionate amount of sodium to the samples which would impact soil health. The saturated paste extract for calcium, magnesium, sodium and SAR method was followed (Miller at al., 2013). Samples were diluted with hydrochloric acid (HCl) at a ratio of 1:9 before testing. Equation 9 was used to calculate soil SAR.

Equation 9 SAR calculation

$$SAR = \frac{Na}{\left(\frac{Ca + Mg}{2}\right)^{0.5}}$$

SAR = sodium adsorption ratio

Na = sodium concentration (mmol/L)

Ca = calcium concentration (mmol/L)

Mg = magnesium concentration (mmol/L)

Total carbon and nitrogen were measured using a FLASH 2000 organic element analyzer (Thermo Fisher Scientific, Massachusetts, United States). Samples were oven dried at 50°C for 24 hours, rolled for 24 hours, and sieved through a 250 μm sieve before being analyzed.

Data Analysis

Statistical Analysis was completed using R version 4.2.1. The treatment groups, denoted as "C", "L", "F", or "S" corresponding to the treatments as shown in Table 5, were compared with the other treatment groups as well as base conditions from the initial soil samples ("IN"). Shapiro-Wilks normality tests were completed to confirm normality of the samples. One-way analysis of variance (ANOVA) statistical testing was then used to determine the significance of the differences between treatments. Data which did not pass the Shapiro-Wilks normality test was instead analyzed with a Kruskal Wallis rank sum test. Results were considered significant if $p < 0.05$. Post-hoc analysis on ANOVA results was completed using Tukey's Range Test. Post-hoc analysis on Kruskal Wallis rank sum tests was completed using a Dunn test with a Bonferroni adjustment. Regression analysis was carried out to understand correlations between different variables. When conducting regression on the S samples, the first two samples from both S1 and S2 were excluded from the regression analysis because the water bypassed the samples during those two weeks resulting in data that was not meaningful. F-tests were completed on the regression models

to determine if the correlation between the independent and dependent variables were significant. Results were considered significant if $p < 0.05$. Geochemists Workbench (GWB) React 2021 was used to model soil solution chemistry. The DI water chemistry and quantity added throughout the experiment was added to the model. The calculated concrete compound quantities which included portlandite, C-S-H, ettringite, calcite, quartz, KOH, $MgOH^+$, and NaOH were added to the model as reactants. The program was run five times, each time varying the amount of the concrete compounds to simulate different concrete amounts. The amounts of concrete simulated included 50 g, 130 g, 500 g, 750 g, and 1000 g.

Because of the inconsistencies in air sample testing, the data was not analyzed. The raw data can be seen in Appendix B.

Chapter 4: Measurement and Modeling of Carbon Sequestration from Concrete Weathering in Soil

Only certain components in concrete capture CO_2 when weathered. These components, shown in Table 6, follow the dissolution chemistry from Equation 1, Equation 3, Equation 4, and Equation 5. Using these equations, it was possible to isolate constituents in the leachate as indicators of concrete carbonation. This chapter aims to quantify the amount of CO_2 captured from concrete carbonation using the calcium, silica, and sulfate in the leachate as proxy data.

Table 6 Components in concrete which sequester CO_2 when weathered and compounds measured in leachate from weathering columns as evidence for weathering

Concrete component	Measurable compounds in water as evidence of weathering
Portlandite	n/a
C-S-H	H_4SiO_4, $H_3SiO_4^-$
Ettringite	SO_4^{2-}
Calcite	Ca^{2+}

Silica

Silica in the leachate is believed to be predominately from the weathering of the C-S-H in concrete. The range of silica in the leachate can be seen in Figure 7. The C samples had the least amount of silica, with concentrations ranging from 0 ppm to 3 ppm. The S samples had silica concentrations greater than the C samples, with concentrations ranging

from 0 ppm to 10 ppm. The L and F samples had the highest amounts of silica, with the L samples ranging in concentration from 4 ppm to 13 ppm and the F samples ranging in concentration from 4 ppm to 22 ppm.

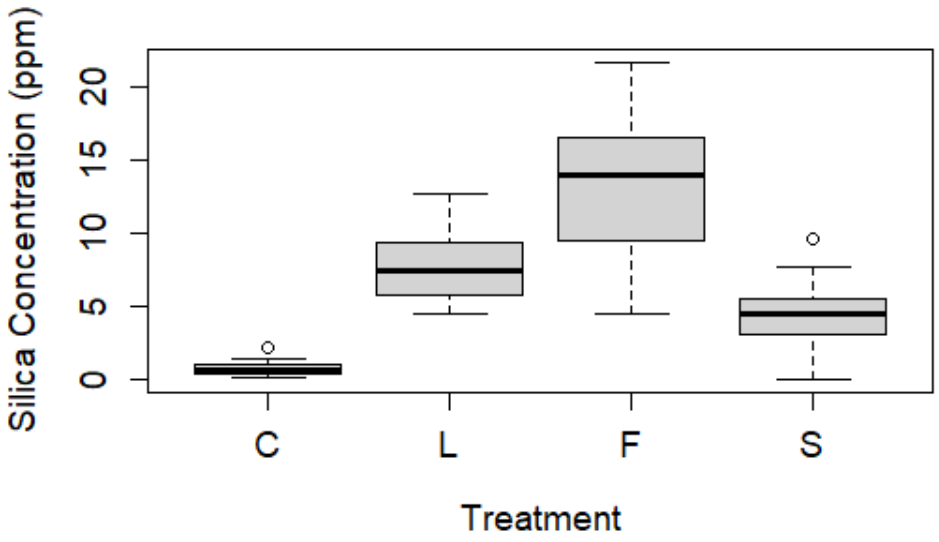

Figure 7 Range of leachate silica concentrations, with "C" being the concrete only samples, "L" being the samples with large concrete fragments in soil, "F" being the samples with small concrete fragments in soil, and "S" being the soil only samples.

The concentration of silica in the majority of the leachate decreased over time, typically beginning with a peak concentration, and then decreasing until leveling off. This could be a result of a quick release of silica followed by the soil solution becoming saturated causing the formation of minerals, leaving the silica concentration in the leachate at equilibrium. It also could be that silica on the concrete surface was more readily available to weather and as time went on the weatherable surface silica decreased. This would align with Thornbush and Viles (2007) who found that newer materials are more susceptible to weathering. On the contrary, all four of the F samples increased in silica over time. The F samples may

have been releasing silica at a faster rate than the rate of mineral formation, causing the solution to be oversaturated with silica. Figure 8 shows the change in silica concentration over time.

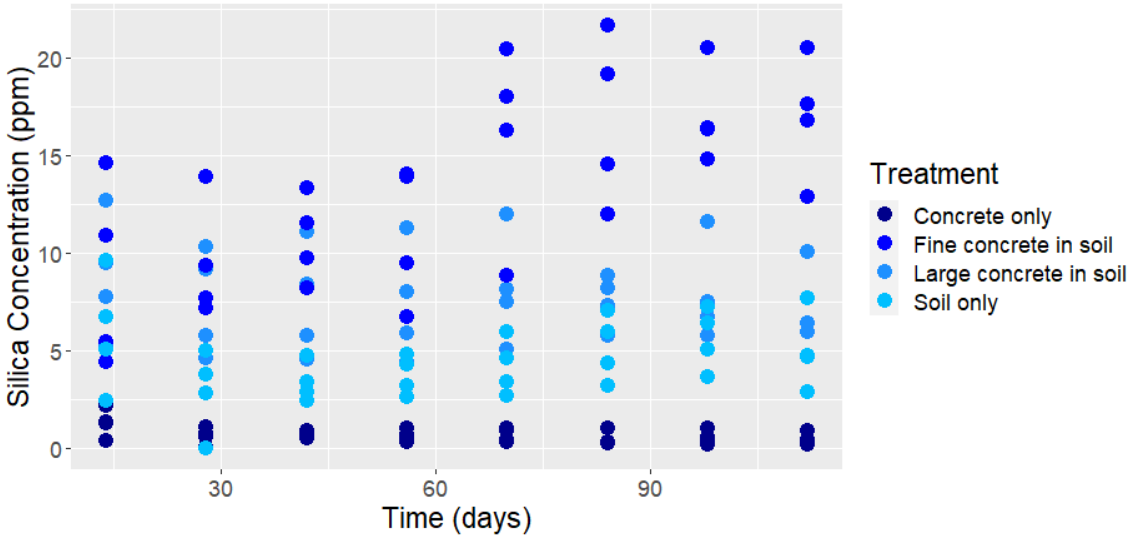

Figure 8 Silica concentration of leachate over the duration of the experiment.

ANOVA statistical testing was used to determine the significance of the silica results. Shapiro-Wilks normality tests were completed first to confirm normality of the samples. The C samples had very little silica and the data did not pass the normality test, so it was not included in the ANOVA analysis. Significant differences were found between the S- L ($p < 0.00049$), S-F ($p < 4.89E-10$) and L-F ($p < 2.02E-9$) treatments, shown in Figure 9. Based off this data, it can be assumed that C-S-H weathered rapidly in the L and F samples which caused a significant increase in silica concentrations, and because of the dissolution equation of C-S-H, CO_2 is being captured from this process.

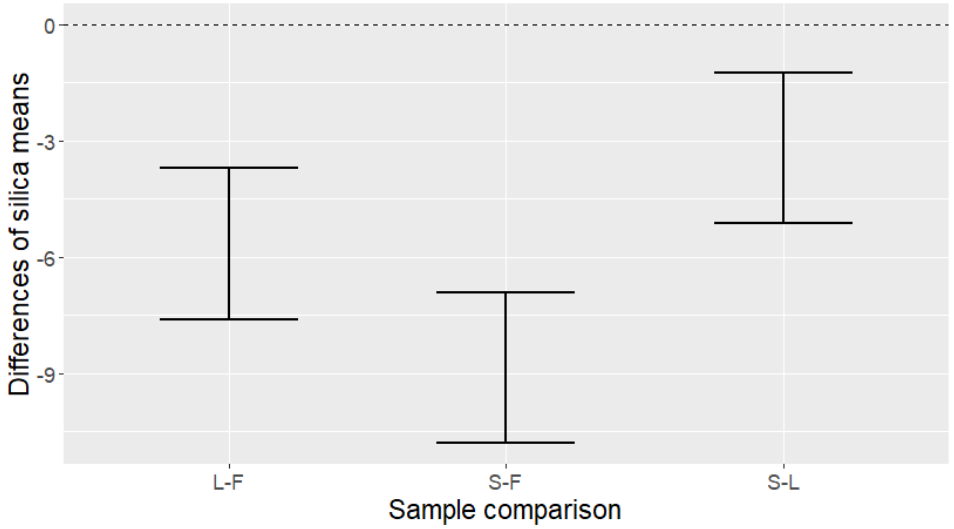

Figure 9 Silica leachate Tukey plot with "L" being the samples with large concrete fragments in soil, "F" being the samples with small concrete fragments in soil, and "S" being the soil only samples. Ranges that include 0 are considered insignificant.

A linear regression analysis of the silica concentrations over time did not yield any meaningful trends. However, a linear regression analysis of the cumulative silica concentrations over time, seen in Figure 10, yielded noticeable trends. This strong correlation between time and cumulative silica concentrations means that the silica being added to the sample every watering event is relatively consistent. The C, L, and S samples had moderate correlations with time, with R^2 values of 0.49, 0.69, and 0.62, respectively. The F samples had a strong correlation with time, with an R^2 value of 0.89. This would fit with the idea that the soil solution reached equilibrium and precipitated excess silica. The L and C samples contain the same sized concrete fragments, but the C samples contain on average about 8.5 times more concrete by weight. However, the L samples had significantly more silica than the concrete samples which is likely due to an increased

weathering rate of C-S-H caused by the soil environment. The slope of the F regression is almost exactly twice the slope of the L regression, with F samples having a slope of 0.55 and L samples having a slope of 0.3. This means that the F samples are weathering almost twice the amount of silica every sample period compared to the L samples. This may be because both solutions are at equilibrium, but the excess silica in the F samples cannot be mineralized quickly enough and the soil solution is instead oversaturated. This difference in weathering rate is likely caused by the difference in fragment size, supporting the hypothesis that the smaller sized fragments will weather at faster rates. All four treatments had F-tests with $p < 0.05$ indicating a statistically significant correlation between time and the cumulative silica concentration in the leachate.

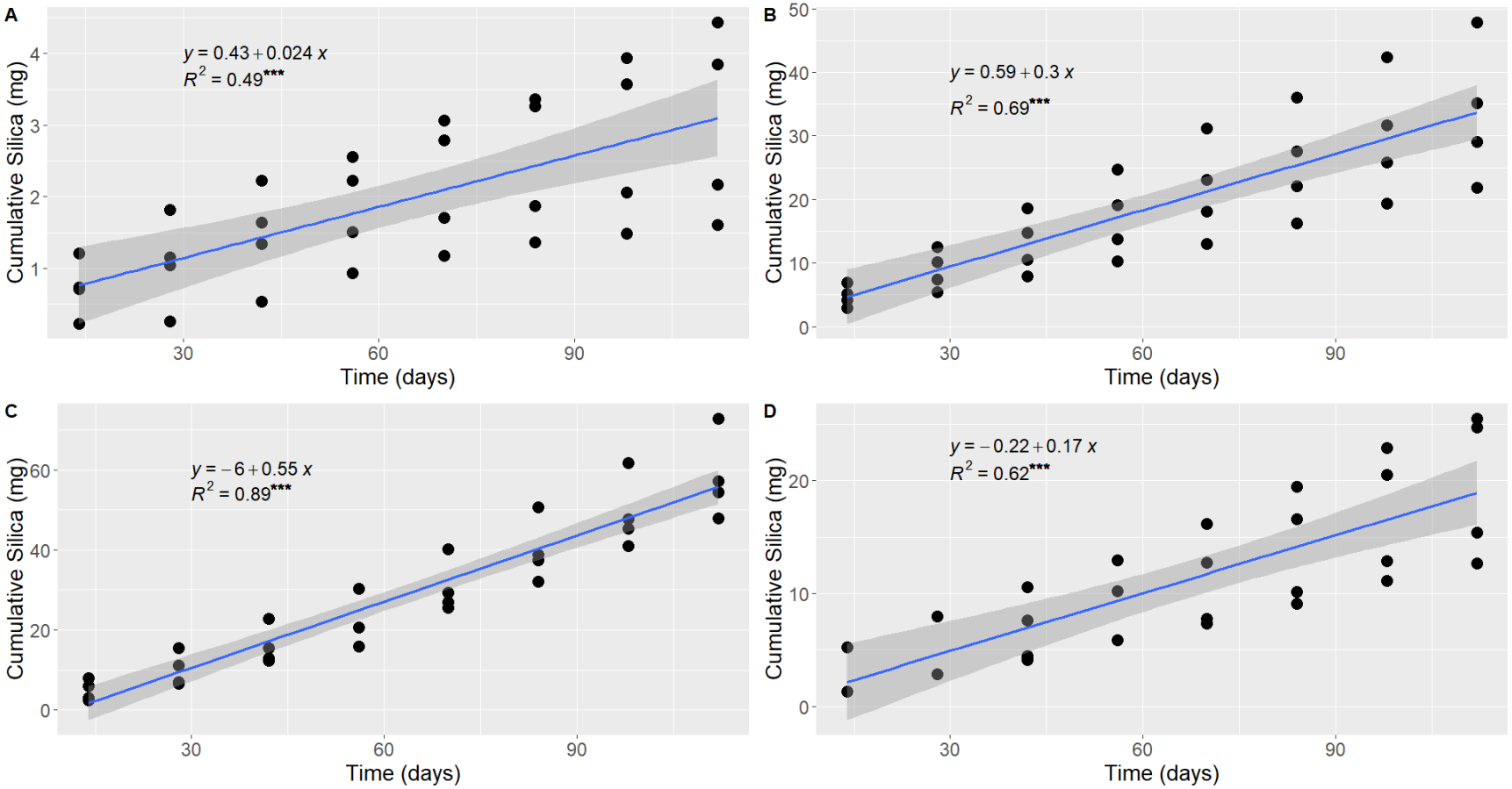

Figure 10 Regression analysis of cumulative leachate silica concentrations versus time with each graph representing a different treatment. (A) C treatment, (B) L treatment, (C) F treatment, and (D) S treatment. Asterisks signify a $p < 0.05$ for the F-test, indicating a statistically significant correlation between the independent and dependent variable.

In alkaline environments, the rate of silicate mineral dissolution typically increases with increasing pH (Brady and Walther, 1989 as cited in Drever, 1993). Figure 11 shows the relationship between the pH values and silica concentrations of the leachate. The S, L, and F samples all appear to see an increase in leachate silica concentration as expected. The C samples do not appear to follow this trend; the silica concentrations remain unchanged with pH. This could be because the water exposure time to the concrete fragments is so short.

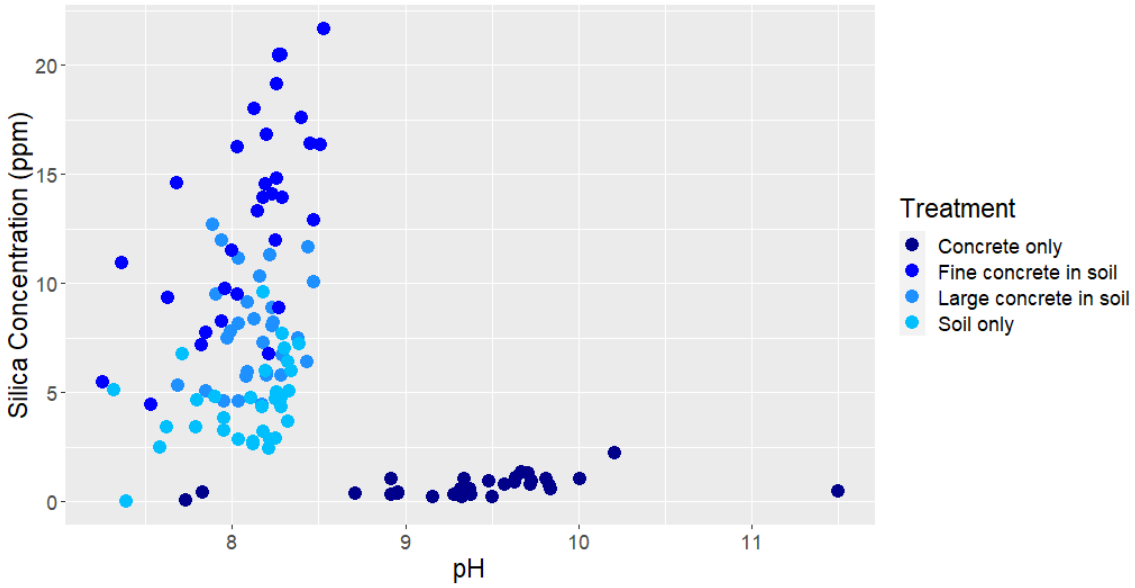

Figure 11 Silica vs. pH of leachate

Calcium

Calcium in the leachate is believed to be sourced from the weathering of the calcite in concrete. Although dissolution equations of other compounds in concrete show calcium being conserved in the formation of calcite, it is possible that some were also sources of calcium. The C samples had calcium concentrations ranging from 2 ppm to 12 ppm. There

was one outlier with a calcium concentration of 37 ppm which belonged to the C4 sample 8; this outlier was likely caused by the increased exposure to water due to the blocked drain. The S and L samples had similar amounts of calcium, with the concentrations in the S samples ranging from 0 ppm to 85 ppm and the L samples ranging in concentration from 22 ppm to 70 ppm. The F samples had much higher amounts of calcium, ranging from 72 ppm to 317 ppm. Figure 12 shows the ranges of calcium concentrations found in the leachate.

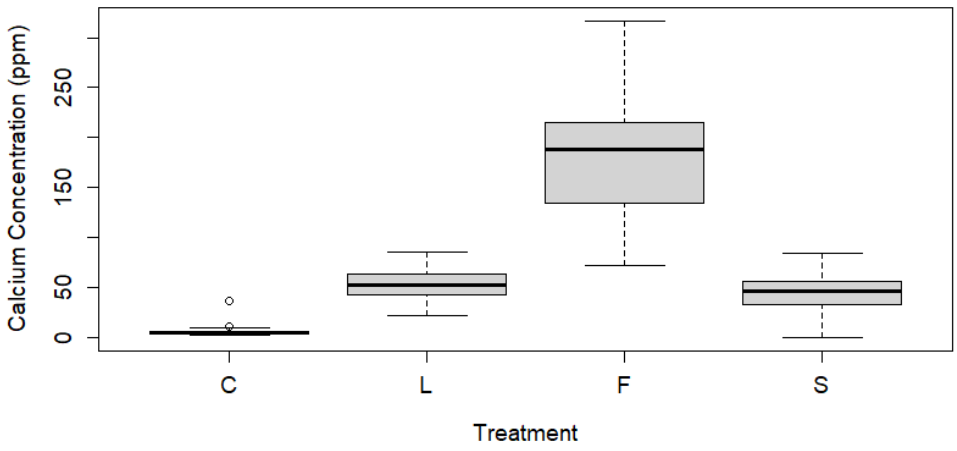

Figure 12 Range of leachate calcium concentrations with "C" being the concrete only samples, "L" being the samples with large concrete fragments in soil, "F" being the samples with small concrete fragments in soil, and "S" being the soil only samples.

The leachate calcium concentrations seemed to increase, hit a peak, and then decrease, as shown in Figure 13. This peak appeared around weeks 10 and 12 for the F samples, but closer to weeks 12 and 14 for the other treatments. It is possible that the soil solutions became saturated with calcium and began precipitating a calcium mineral. Calcium could have entered the solution quickly, oversaturating the solution before minerals began precipitating, which is why the peak occurs and then the concentration decreases.

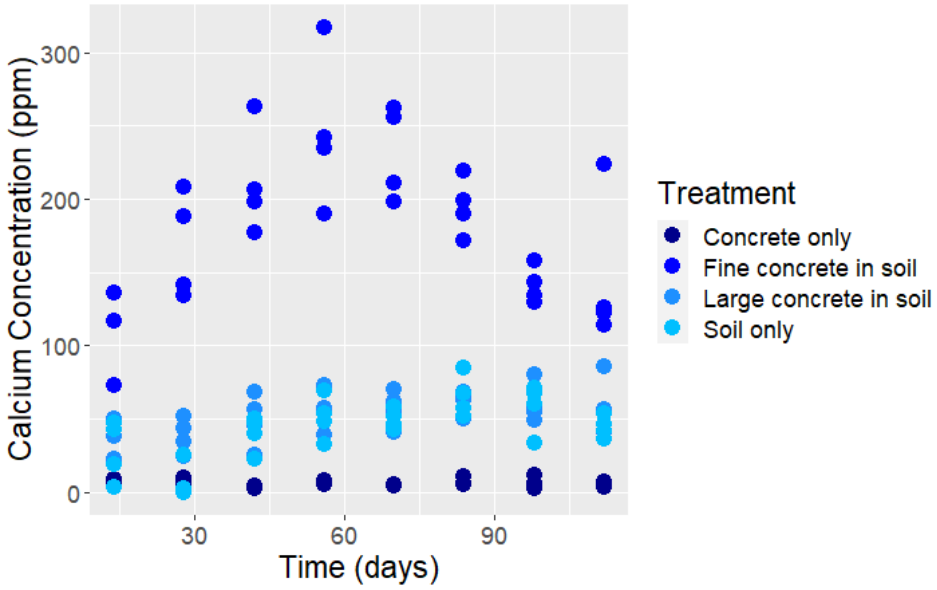

Figure 13 Calcium concentration of leachate over the duration of the experiment.

ANOVA statistical testing was used to determine the significance of the calcium results. Shapiro-Wilks normality tests were completed first to confirm normality of the samples. The C samples had very little calcium and the data did not pass the normality test, so it was not included in the ANOVA analysis. Significant differences were found between the S-F ($p < 4.89E-10$) and the L-F ($p < 4.89E-10$) treatments, but not between the S and L treatments; this can be seen in Figure 14. This lack of significance between the S and L samples indicates that the calcium may be coming from material already in the soil and that calcite is not weathering as quickly in the L samples compared to the F samples. The lack of significance could also be explained by excess calcium being captured by the CEC, minimizing the calcium in the leachate. This again supports the hypothesis that the smaller

concrete fragments in the F sample are weathering faster. This also indicates that C-S-H weathers faster than calcite.

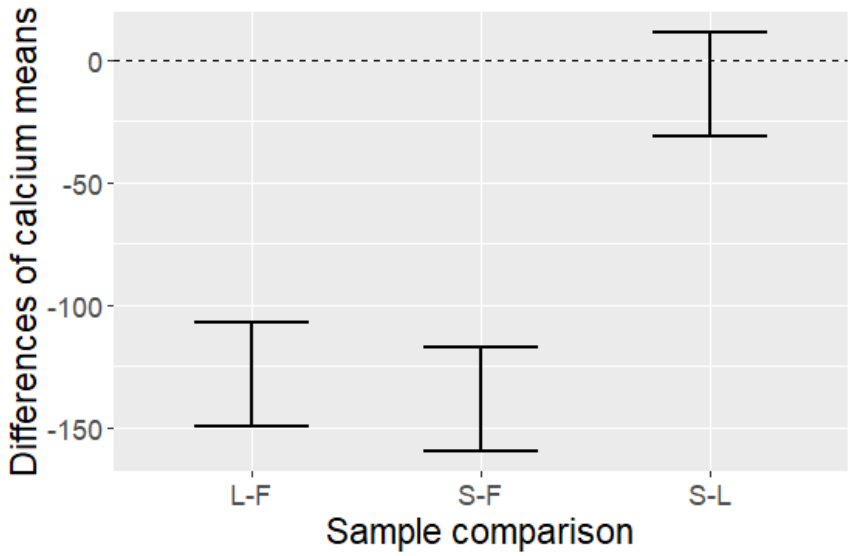

Figure 14 Calcium leachate Tukey plot with "L" being the samples with large concrete fragments in soil, "F" being the samples with small concrete fragments in soil, and "S" being the soil only samples. Ranges that include 0 are considered insignificant.

A linear regression analysis of the calcium concentrations over time did not yield any meaningful trends. However, a linear regression analysis of the cumulative calcium concentrations over time, seen in Figure 15, yielded noticeable trends. The L and C treatments both had R^2 values 0.85 and the F and S treatments both had R^2 values of 0.93. This strong correlation between time and cumulative calcium concentrations means that the calcium being added to the sample every watering event is relatively consistent. The strong correlation in the samples with soil is probably caused by a few different factors. One may be due to the soil cation exchange capacity (CEC) capturing calcium and regulating how much is being released. Another reason may be that the calcium in solution

reached equilibrium and any excess calcium being released is forming minerals. Again, the L samples have a much larger slope than the C samples, and the F samples have a much larger slope than the L samples; this shows that concrete in soil is weathering faster than the concrete alone, and the smaller concrete fragments are weathering at a faster rate compared to the larger fragments. All four treatments had F-tests with $p < 0.05$ indicating a statistically significant correlation between time and the cumulative calcium concentration in the leachate.

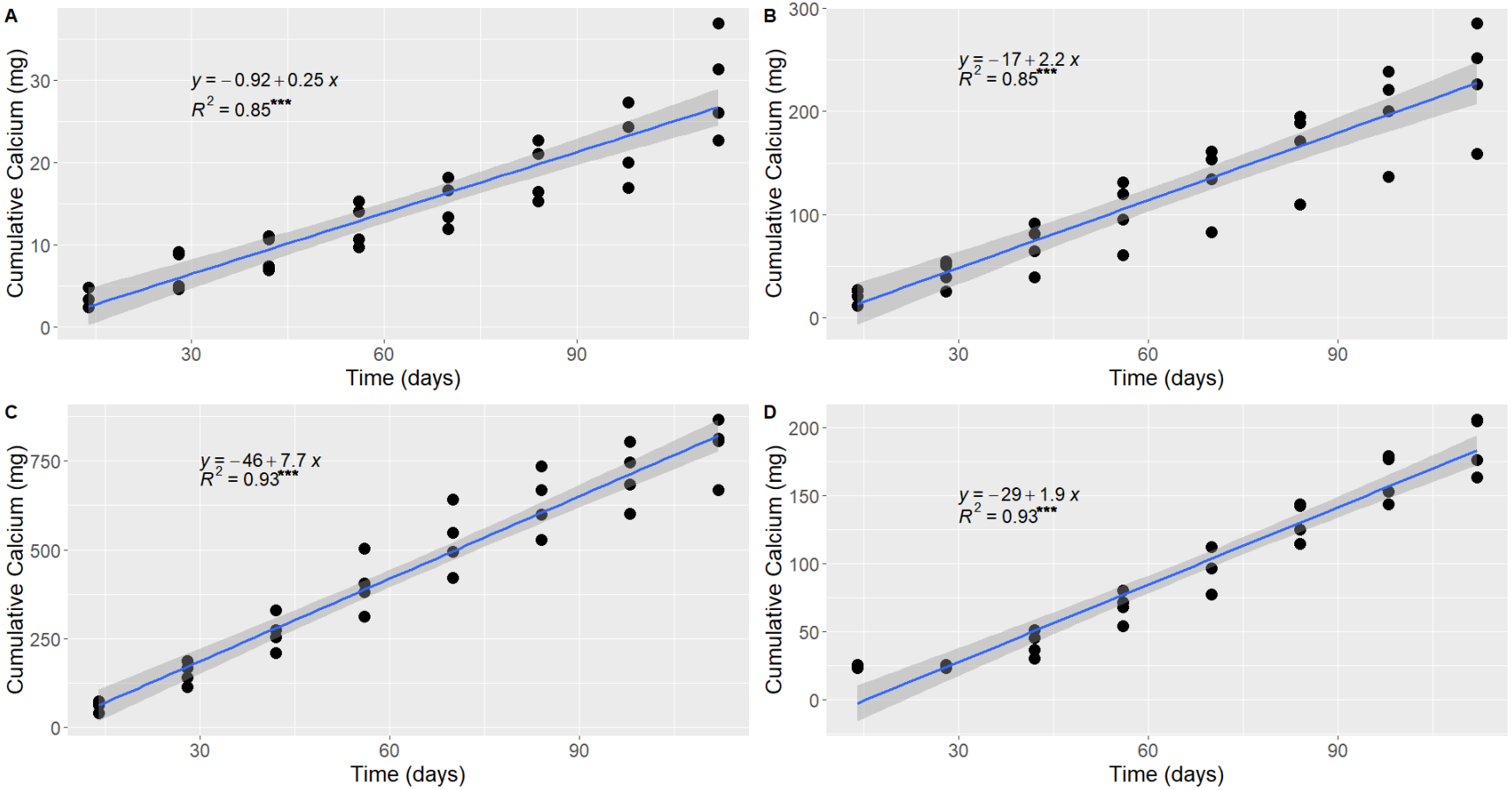

Figure 15 Regression analysis of cumulative leachate calcium concentrations versus time with each graph representing a different treatment. (A) C treatment, (B) L treatment, (C) F treatment, and (D) S treatment. Asterisks signify a $p < 0.05$ for the F-test, indicating a statistically significant correlation between the independent and dependent variable.

Sulfate

Sulfate in the leachate is believed to be sourced from the weathering of the ettringite in concrete. The S and C samples had similar calcium concentrations, ranging from 0 ppm to 15 ppm and 0 ppm to 12 ppm respectively. Comparatively, the L samples had elevated sulfate concentrations that ranged from 5 ppm to 43 ppm. The F leachate had extremely high sulfate concentrations, ranging from 23 ppm to 526 ppm with an outlier of 0 ppm believed to be an error. Figure 16 shows the range of values of the sulfate concentrations in the leachate.

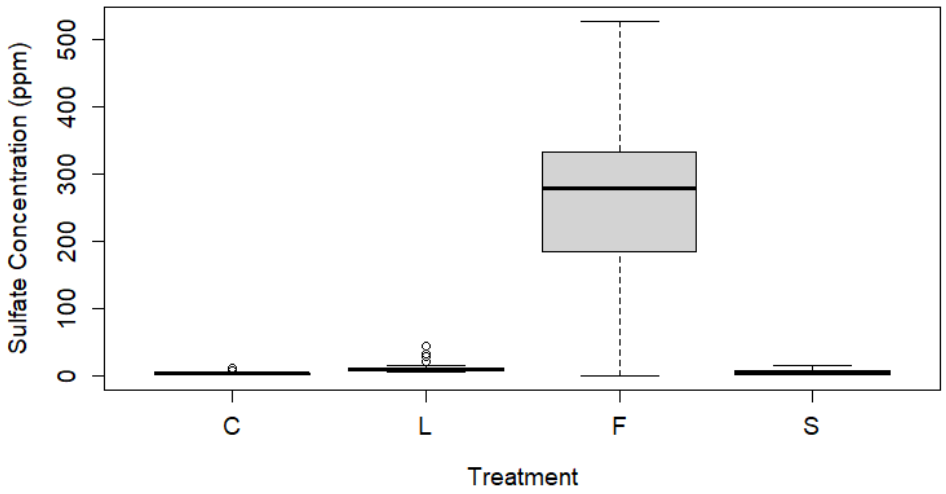

Figure 16 Range of leachate sulfate concentrations with "C" being the concrete only samples, "L" being the samples with large concrete fragments in soil, "F" being the samples with small concrete fragments in soil, and "S" being the soil only samples.

The sulfate concentrations of the leachate varied during the course of the experiment, shown in Figure 17. Similar to calcium, the sulfate concentrations of the F samples seemed to increase, hit a peak, and then decrease. The majority of the other samples decreased with

time, beginning with a peak concentration and then decreasing steadily and leveling off. Like calcium and silica, it's possible that the soil solution because saturated and began precipitating sulfate minerals. It could also be that that newer materials were more susceptible to weathering per Thornbush and Viles (2007).

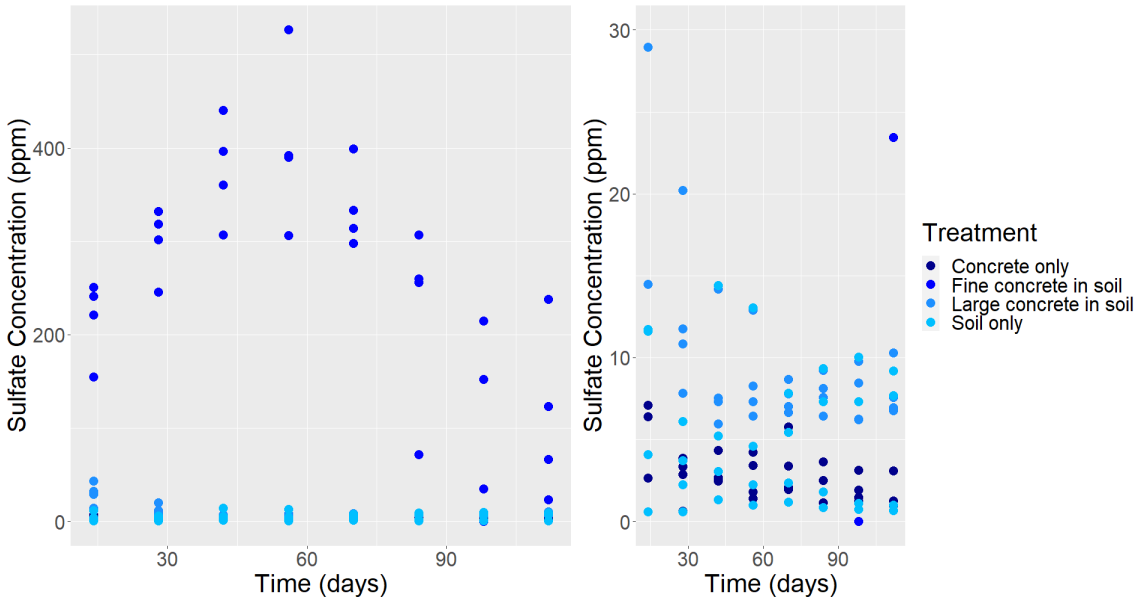

Figure 17 Sulfate concentration of leachate over the duration of the experiment. The image on the left shows all sample data; the image on the right has been restricted on the y-axis to better represent the smaller values.

ANOVA statistical testing was used to determine the significance of the sulfate results. Shapiro-Wilks normality tests were completed first to confirm normality of the samples. The F samples were the only treatment to pass the normality test, so instead a Kruskal Wallis rank sum test was completed. The Kruskal Wallis rank sum test found a $p < 2.2E-16$, confirming significance of the results. A post-hoc analysis was performed using a Dunn test with a Bonferroni adjustment.

Table 7 shows the results from the Dunn test; every comparison was significant except the S-C pair. This data supports the concept that ettringite weathered rapidly in the L and F samples and caused a significant increase in silica concentrations. Because of the dissolution equation of ettringite, it is believed that CO_2 is being captured from this process.

Table 7 Post-hoc Dunn test of sulfate values with "C" being the concrete only samples, "L" being the samples with large concrete fragments in soil, "F" being the samples with small concrete fragments in soil, and "S" being the soil only samples.

Comparison	F-C	L-C	S-C	L-F	S-F	S-L
p-value	5.4E-16	4.5E-5	1	0.00074	3.6e-12	0.00463

Again, a linear regression analysis of the sulfate concentrations over time did not yield any meaningful trends, but a linear regression of the cumulative sulfate concentrations over time did, seen in Figure 18, signaling that the amount of sulfate weathering after each watering event is relatively consistent. The S sample had a weak correlation between time and cumulative sulfate, with an R^2 value of 0.35. This is not surprising as the source of sulfate is believed to be from the ettringite in concrete. The C and L samples had moderate correlations, with R^2 values of 0.57 and 0.64 respectively while the F samples had a high correlation of 0.9. The L samples are weathering at a rate three times that of the C samples even though the C samples have 8.5 times more concrete, leading to the conclusion that the soil is facilitating faster weathering of the ettringite. The F samples are weathering at a rate 33 times faster than the L samples, again supporting the hypothesis that the smaller fragments are weathering at a faster rate. All four treatments had F-tests with $p < 0.05$

indicating a statistically significant correlation between time and the cumulative sulfate concentration in the leachate.

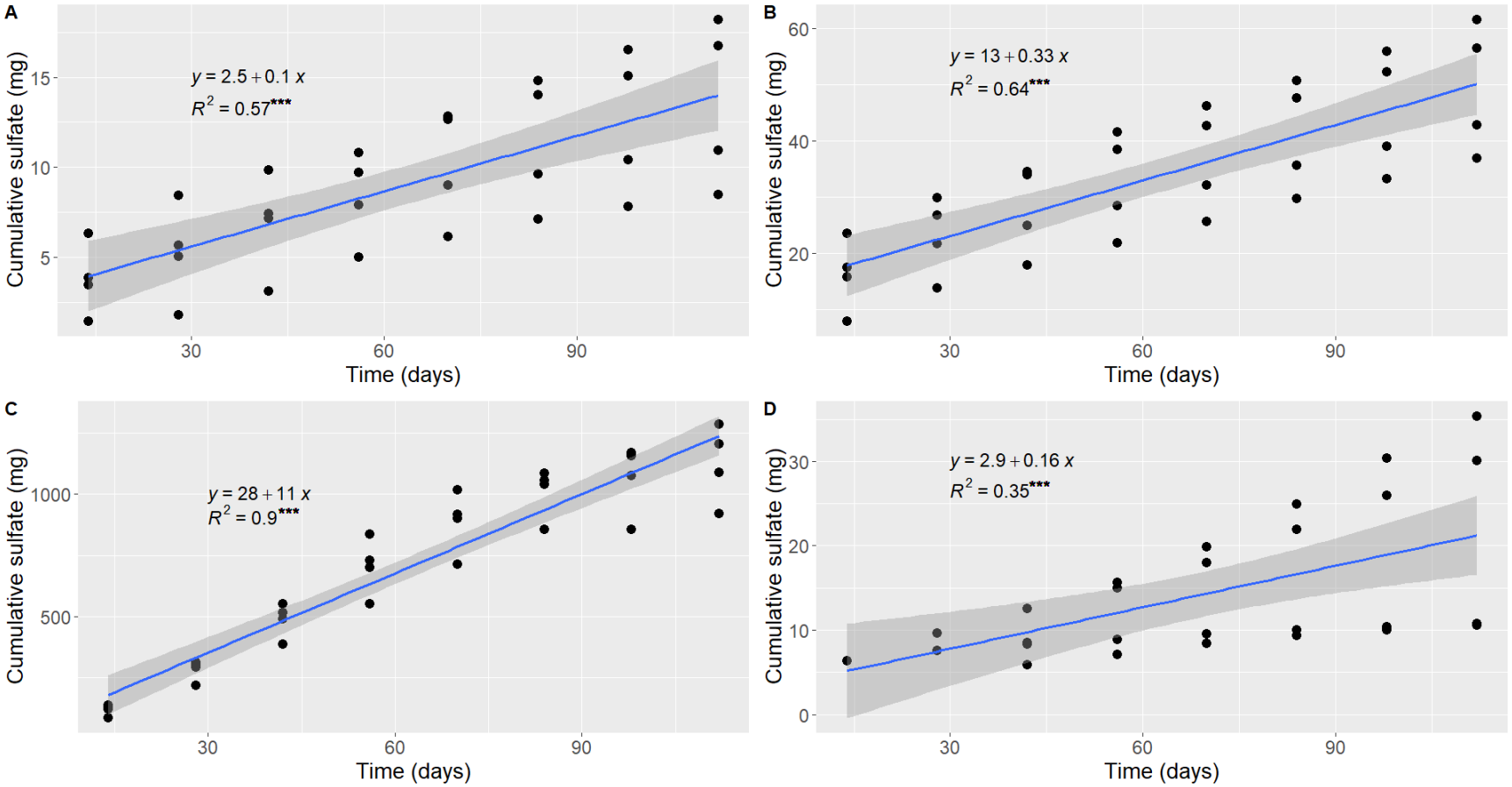

Figure 18 Regression analysis of cumulative leachate sulfate concentrations versus time with each graph representing a different treatment. (A) C treatment, (B) L treatment, (C) F treatment, and (D) S treatment. Asterisks signify a $p < 0.05$ for the F-test, indicating a statistically significant correlation between the independent and dependent variable.

X-Ray Diffraction

X-ray diffraction (XRD) data did not show clear evidence supporting the formation of pedogenic carbonates from concrete carbonation. No carbonates were detected in the L treatment samples; however, it is possible that pedogenic carbonates were formed but the small sample tested was not representative of the sample as a whole. Calcite and dolomite were both detected in the F samples, however the concrete fragments in these samples could not be separated out due to their small size. Therefore, it is unknown if the calcite and dolomite detected are secondary carbonates formed from concrete carbonation or unreacted concrete.

Modeling

Modeling was completed to predict the amount of carbon sequestered from concrete carbonation. The cumulative silica, sulfate, and calcium masses in the leachate from the duration of the experiment were used. From Figure 19 it can be seen that calcium, silica, and sulfate are all positively correlated, presumably because larger amounts of one would indicate more concrete carbonation, in turn yielding higher amounts of the other two.

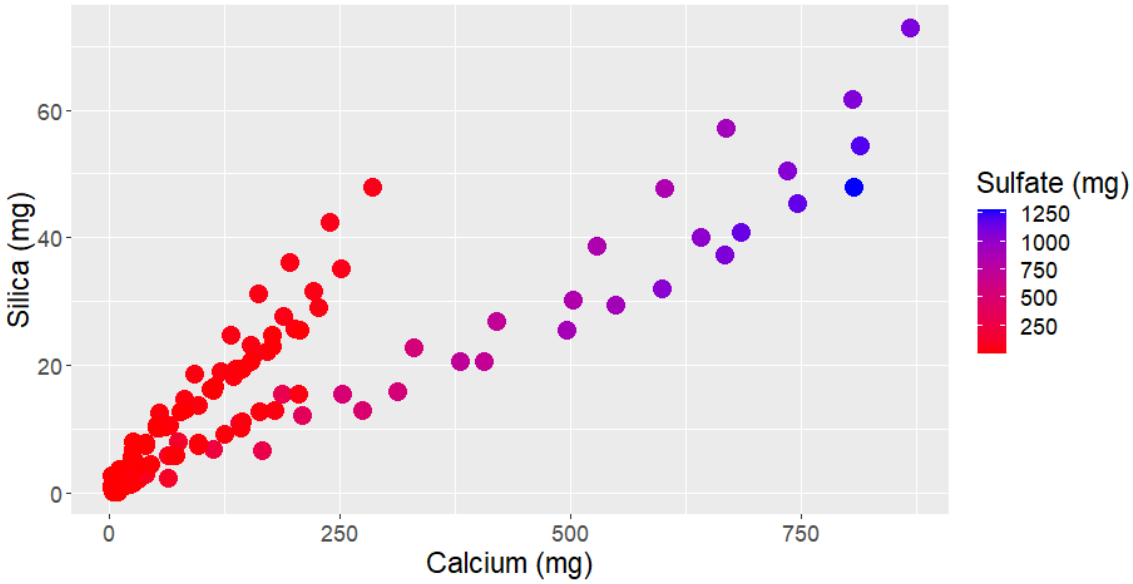

Figure 19 Measured leachate cumulative calcium vs. silica vs. sulfate

In order to negate any constituents contributed from the soil, the average of the S treatments was subtracted from each concentration. Stoichiometry was then utilized with Equation 1, Equation 4, and Equation 5 to calculate the amount of CO_2 captured from the reaction. For ease of calculations, only Equation 4c was used as the dissolution reaction for C-S-H. Equation 10 is the general equation followed to calculate the mass of CO_2 from the masses of silica, sulfate, and calcium.

Equation 10 Example calculation of CO_2 from calcium

$$CO_2(g) = \frac{Ca^{2+}(g)}{molar\ mass\ of\ Ca^{2+}\ (\frac{g}{mol})} * \frac{1\ mol\ CO_2}{1\ mol\ Ca^{2+}} *\ molar\ mass\ of\ CO_2\ (\frac{g}{mol})$$

The amount of CO_2 captured from the weathering of portlandite was difficult to quantify because there was not a direct measurement that could be used. Figure 20 shows that the relationship between silica and sulfate is linear, and the C, L, and F treatments had F-tests with $p < 0.05$ indicating a statistically significant correlation between cumulative sulfate concentration and cumulative silica concentration. The S treatment did not have a statistically significant correlation between these two values. This suggests that the major source of the silica and sulfate in the samples was concrete, hence why the S samples did not have this correlation. It also leads to the conclusion that concrete is weathering at a consistent rate. Because of this, ettringite and C-S-H, both also components of cement paste, were used as proxy data to estimate the amount of portlandite that weathered.

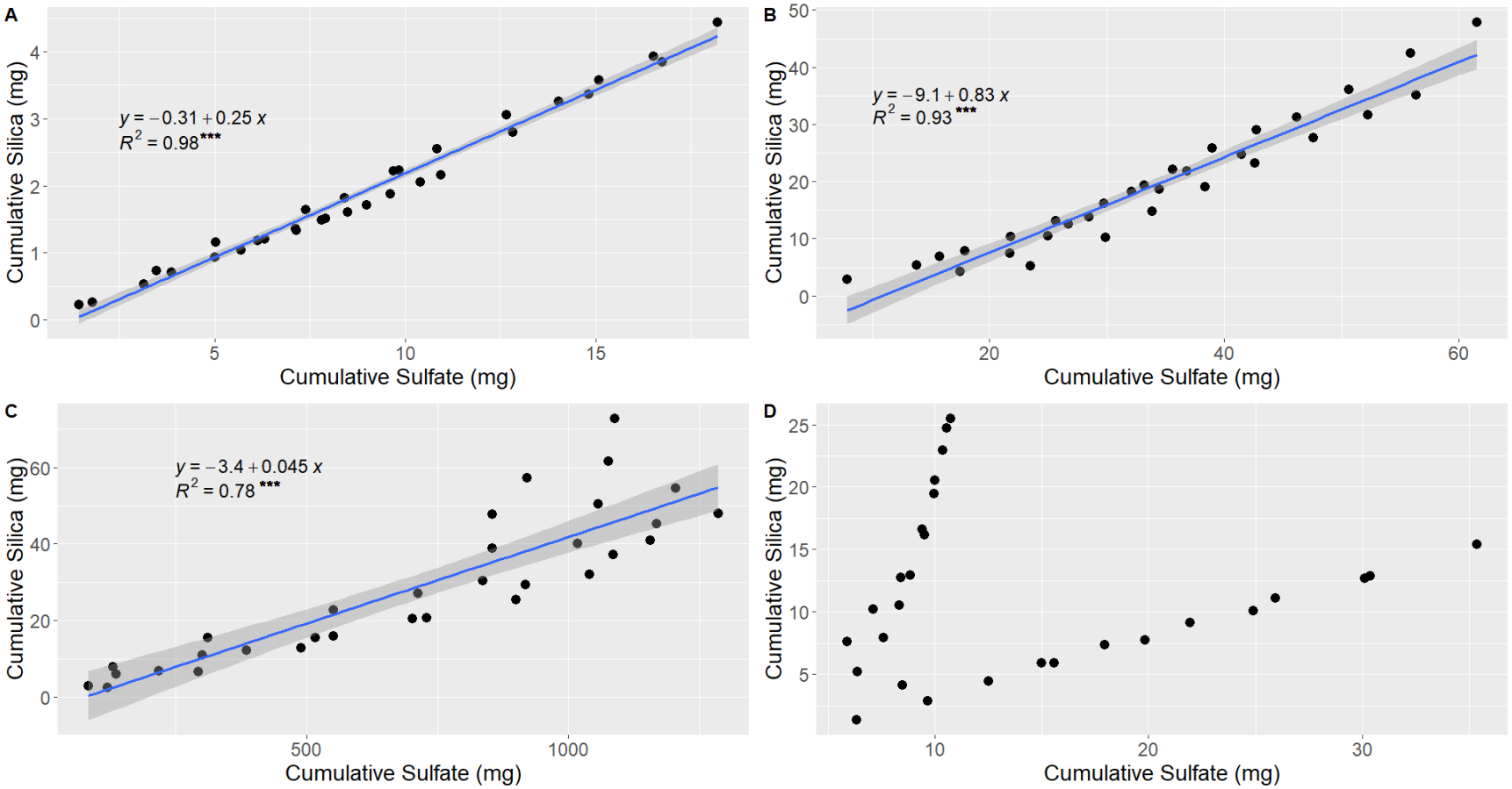

Figure 20 Regression analysis of cumulative leachate sulfate concentrations versus cumulative leachate silica with each graph representing a different treatment. (A) C treatment, (B) L treatment, (C) F treatment, and (D) S treatment . Asterisks signify a $p < 0.05$ for the F-test, indicating a statistically significant correlation between the independent and dependent variable.

First, the percentage of each component in concrete was calculated. This was done by multiplying the concrete mix design quantities and the known percentages of each compound in cement paste or cement. Table 8 shows the final compound percentages used for calculations.

Table 8 Concrete component percentages

Concrete compound	% of concrete*
Portlandite	6.48**
C-S-H	15.56**
Ettringite	3.89**
MgO	0.45***
K_2O	0.11***
Na_2O	0.06***
$CaCO_3$	42.7%
SiO_2	31.2%

*Totals to 100.59% because values acquired from different sources
**Calculated using Saleh and Eskander, 2020
*** Calculated using Saleh and Mindess et al., 2003

Using the above values, the mass of sulfate or silica was used to determine how much concrete total should have reacted to produce those masses. The total amount of concrete could then be multiplied by the amount of portlandite expected in concrete and then the dissolution equation used to calculate grams of CO_2 used in the reaction. Equation 11 shows an example calculation to calculate the amount of CO_2 captured from the weathering of portlandite using the measured SO^{4-} mass.

Equation 11 Example calculation of CO_2 from portlandite using measured SO^{4-}

$$CO_2(g) = \frac{measured\ SO^{4-}\ (g)}{molar\ mass\ of\ SO^{4-}(\frac{g}{mol})} * \frac{moles\ of\ ettringite}{moles\ of\ SO^{4-}} * \frac{1}{0.1556} * 0.0648$$

$$* \frac{moles\ of\ CO_2}{moles\ of\ portlandite} *\ molar\ mass\ of\ CO_2\ (\frac{g}{mol})$$

The amount of CO_2 captured from the weathering of portlandite was calculated using both silica and sulfate values for all samples; these two values were then averaged to get the mass of CO_2 from weathered portlandite. The CO_2 values calculated from all four compounds were added together to get the total amount of CO_2 captured by each sample. Figure 21 shows the relationship between concrete weight in the samples versus the amount of CO_2 the samples sequestered in the testing period which simulated one year.

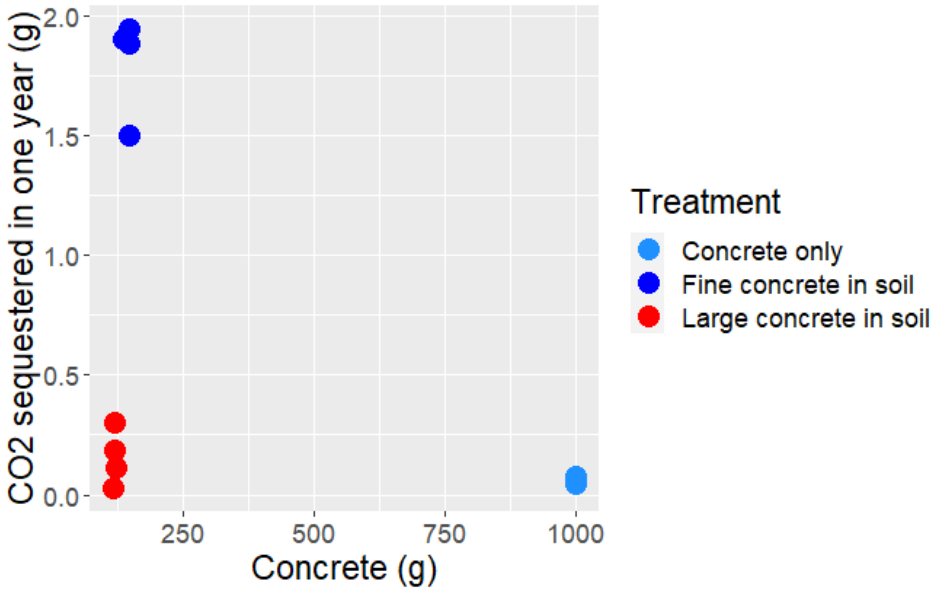

Figure 21 Concrete weight vs. CO2 sequestered in one year

Because the concrete fragments varied in size, directly comparing the quantity of concrete and the carbon captured would not yield accurate results. To correct for this, the concrete surface area was instead calculated. Fragments were assumed to be perfect spheres with diameters of either 8 mm or 0.48 mm; these values were used to calculate the surface area and volume of one concrete fragment. The density of the concrete was determined to be 0.0022 g/mm^3 from the mix design quantities, and this was used to calculate the mass of one concrete fragment. Knowing the total concrete weight per sample and the weight of one fragment, the theoretical number of fragments per sample could be calculated. This value was then multiplied by the surface area of one fragment to get the total concrete surface area per sample. An example calculation of the total concrete surface area is given in Equation 12.

Equation 12 Example calculation for concrete surface area

$$total\ \ surface\ area\ = \frac{mass\ of\ concrete\ in\ sample\ (g)}{mass\ of\ one\ particle\ (g)} * (4 * \pi * \left(\frac{8}{2}\right)^2)$$

Figure 22 shows the different treatments, the calculated concrete surface area of each sample, and the calculated CO_2 sequestered in one year by the weathering of that concrete. Although the C treatment had a concrete surface more than eight times that of the L treatment, the C samples sequestered less CO_2. This indicates that concrete in soil weathers at a faster rate making it able to sequester more CO_2.

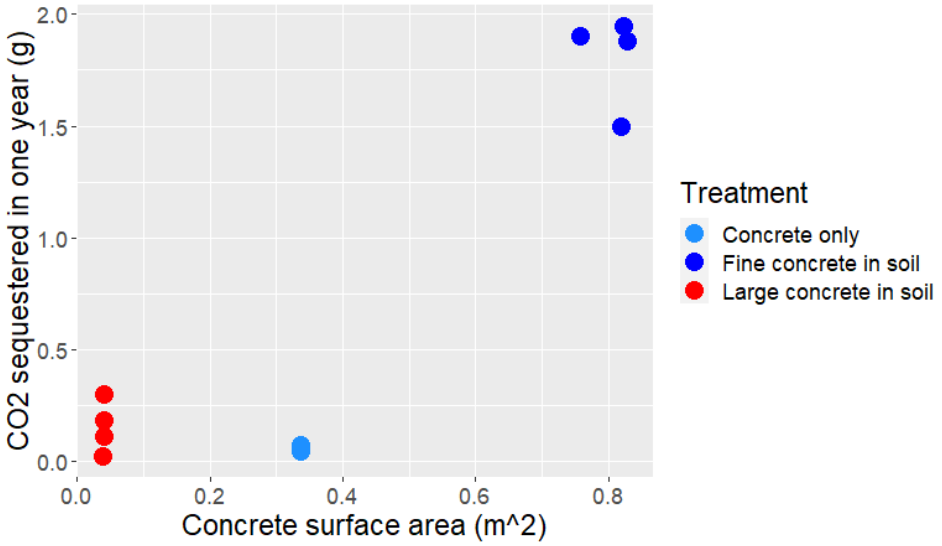

Figure 22 Concrete surface area vs. CO_2 sequestered in one year

Linear regression analysis was completed on the L and F samples to understand the relationship between the amount of CO_2 sequestered and the surface area of concrete in soil. This can be seen in Figure 23. The regression found an R^2 value of 0.96, conveying an extremely high correlation between concrete surface area in soil and carbon sequestration. The model F-test had a $p < 0.05$ indicating a statistically significant correlation between concrete surface area and sequestered CO_2. This relationship could be used to optimize concrete fragment size and carbon sequestration due to the cost/labor of crushing concrete.

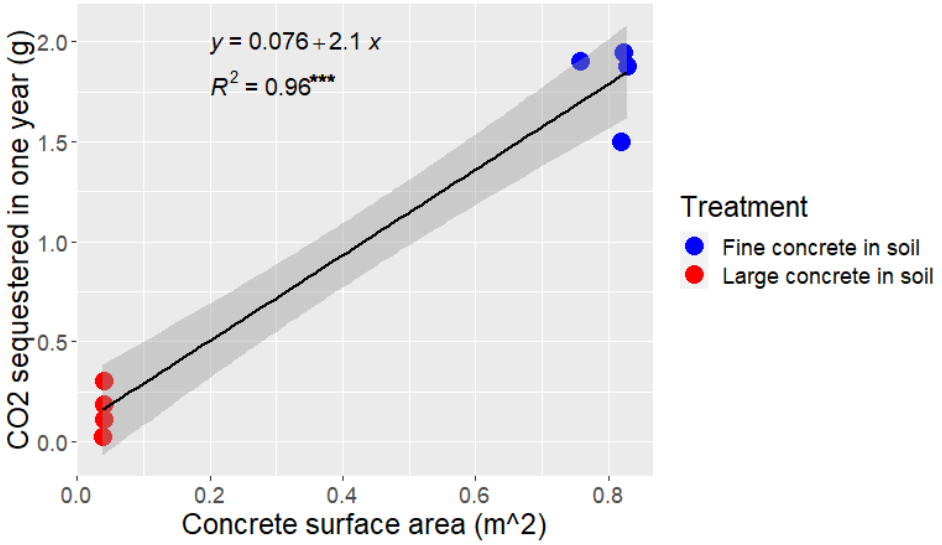

Figure 23 Concrete surface area vs. CO2 sequestered in one year of concrete in soil. Asterisks signify a $p < 0.05$ for the F-test, indicating a statistically significant correlation between the independent and dependent variable.

Table 9 gives a summary of the measured of soil and concrete, the calculated surface areas, and the calculated annual CO_2 sequestered in the treatments.

Table 9 Summary of treatments and annual CO_2 sequestered

	Concrete (g)		Soil (g)		Surface area (g)		CO_2 sequestered annually (g)	
Treatment	Mean	Std Dev	Mean	Std Dev	Mean	Std Dev	Mean	Std Dev
C	1000	-	0	-	0.34	-	0.06	0.01
L	119	3	1075	23	0.04	0.001	0.16	0.10
F	144	5	1295	47	0.81	0.03	1.81	0.18

If the soil solutions became saturated and began precipitating minerals from the excess silica, calcium, and sulfate, then less of those constituents would have appeared in the leachate and the calculated CO_2 captured would be an underestimate. To better understand the solution chemistry, modeling was completed using Geochemists

Workbench (GWB) React program. The deionized water chemistry was added to the program as well as the total water added throughout the experiment and the quantities of the different concrete components per Table 8. The model is different from the actual experiment because it simulates the materials being added to the fluid rather than the fluid passing through the materials, overestimating the exposure time. The model was run with differing amounts of concrete to create a data curve. The resulting water chemistry was then used to calculate the amount of CO_2 that was captured by the reaction as was done to the experimental data using Equation 10. It was not possible to calculate the concrete surface area used in the GWB model because the fragment sizes were unknown. The model F-test had a $p < 0.05$ indicating a statistically significant correlation between concrete mass and sequestered CO_2.

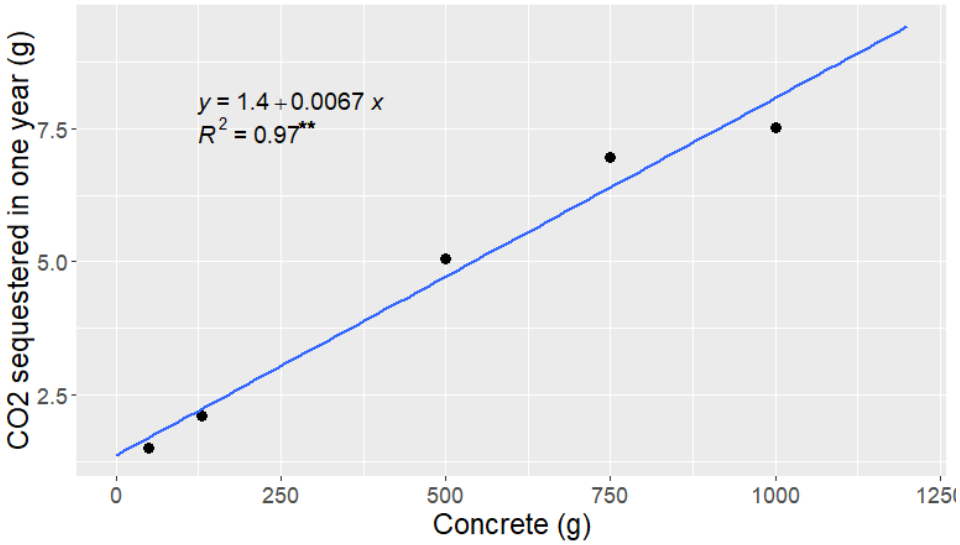

Figure 24 GWB model of CO_2 sequestered using concrete masses of 50, 130, 500, 750, and 1000 g. Asterisks signify a $p < 0.05$ for the F-test, indicating a statistically significant correlation between the independent and dependent variable.

Figure 25 shows the regression line created from the GWB model data and the experimental data on the same plot. The C samples far fall below the models' expected value. The L samples are also below the expected values from the model, but not nearly as much as the C samples. The F samples are less than the predicted values, however they do not vary as much.

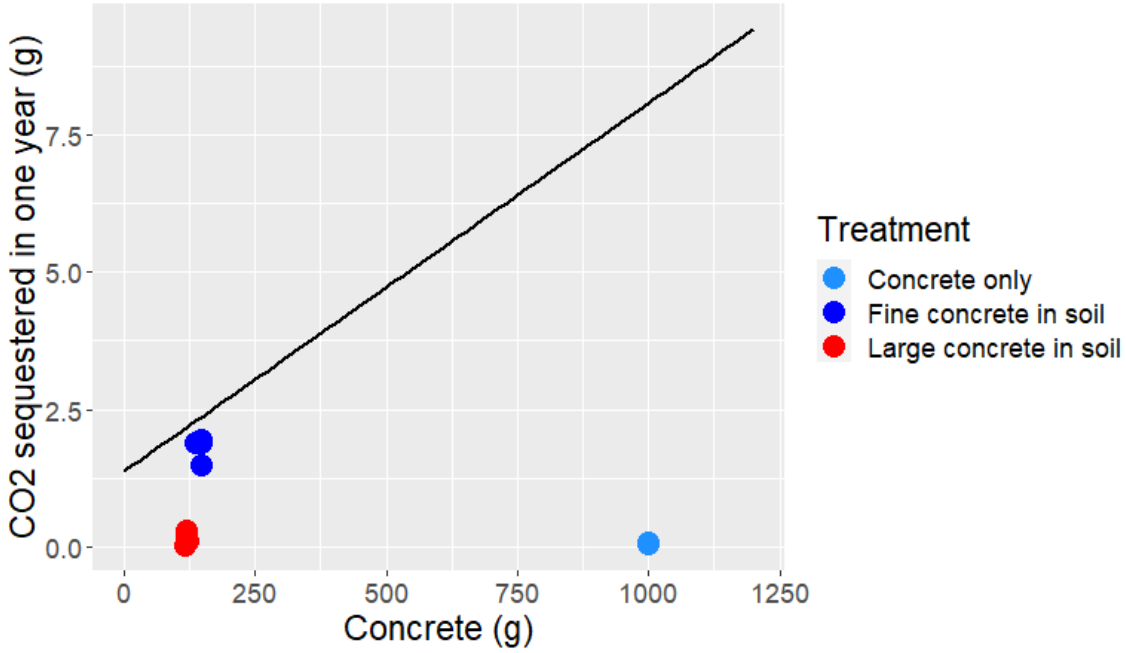

Figure 25 Estimated regression line from GWB compared to calculated experimental data

Several minerals in the model were predicted to be saturated. Table 10 is a list of the minerals predicted to be saturated in the GWB model solution. The other minerals, excluding calcite, all contain both calcium and silica. Because the chemistry of the GWB model differs greatly than the experimental data, these minerals may not have been fully saturated during the experiment. If they were precipitated, the formation of the minerals would have led to the underestimation of the sequestered CO_2.

Table 10 Saturated minerals predicted by the GWB model

Saturated minerals per GWB model	Chemical formula
Prehnite	$Ca_2Al_2Si_3O_2(OH)$
Calcite	$CaCO_3$
Diopside	$MgCaSi_2O6$
$Ca_5Si_6O_{17}^{21}.2H_2$	n/a

Conclusions

- The significant differences between the C samples and the L and F samples are evidence that the soil is facilitating faster concrete weathering rates .
- The significant differences between the L and F samples are evidence that the smaller concrete fragments are weathering faster than the larger concrete fragments.
- This study found that putting 120-150 g of concrete in soil sequestered 0.15-1.8 g of CO_2. Modeling the data, it is predicted that for every 1 m^2 surface area of concrete added to soil, 2.1 g of atmospheric carbon is sequestered annually.
- The predicted amount of CO_2 captured may be an underestimate if the soil solutions were saturated and other minerals formed which distorted the calcium, silica, and sulfate in the leachate that weathered from the concrete.

Chapter 5: Environmental Impacts of Concrete Weathering in Soil

Introducing a new material to an environment will cause changes to the chemical, biological, and physical characteristics of that environment. In the past, damage to nature and humans has been caused due to the introduction of new materials when environmental consequences were not fully understood. It was the intention of this research to explore all possible ecological implications which could come from the introduction of concrete to soil. Notable impacts to soil health, including pH, sodium concentrations, aggregate stability, and microbial well-being, as well as the nitrogen concentration of leachate will be explored in this chapter.

Soil health

pH

pH measurements of the leachate are shown in Figure 26. The DI water added to the columns varied in pH because the time the water was left exposed to the environment prior to collection varied. The pH of the DI water ranged from 5.3 to 6.2 throughout the experiment and did not appear to impact the resulting leachate pHs. The pH of the water changed as it passed through the columns. There was some variation between the leachate pHs of the S, L, and F treatments; the pHs started between 7.2 and 8.2 and slowly increased over time, with the S samples ending at approximately 8.3 and the L and F samples ending

closer to 8.4. It is possible that the soil contained trace amounts of alkaline minerals which increased the leachate pH and impacted all three groups similarly. The final leachate pH values of the L and F samples were slightly higher than the S samples which was likely due to the dissolution of concrete which is alkaline. The pH values of the C samples were considerably higher than the other three treatments, with starting values near 10 and ending values having a large range between 9 and 11.5. It is believed that the organic matter in the soil acted as a buffer in the mixed L and F samples and prevented a larger increase in water pH similar to the C samples. The C samples all followed similar trends, decreasing slightly after the initial sample and then increasing again towards the end of the experiment.

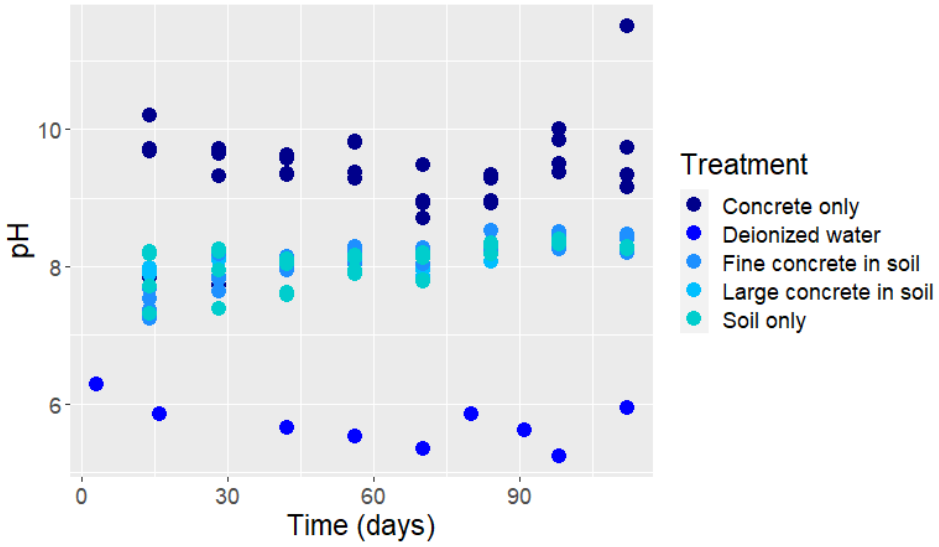

Figure 26 pH of leachate over the duration of the experiment. The sample with pH greater than 11 was caused by a blockage in the tubing which forced water to buildup in the column and increase the exposure time of the water to the concrete.

There was a notable jump in pH for the last measurement of C4. Before this measurement was taken, the tubing leading from the column to the collection cup was

blocked by a precipitate; water had built up into the column and the concrete was submerged for an unknown amount of time. This increased contact with the concrete greatly increased the water pH. This phenomenon has ramifications for concrete added to soils with high moisture retention capabilities. Concrete added to soils with high water holding capacities may see larger increases in soil water pH due to increased contact time with concrete. This also has ramifications outside the scope of this experiment in situations where water on concrete infrastructure is poorly drained. This can impact natural water bodies that collect urban drainage and increase the costs of water treatment.

A Kruskal Wallis rank sum test was used to determine the significance of the leachate pH results because all samples failed the Shapiro-Wilks normality tests except the F samples. The Kruskal Wallis rank sum test found a $p < 2.8E\text{-}12$, indicating significance of the results. A post-hoc analysis was performed using a Dunn test with a Bonferroni adjustment. The L, S, and F treatments were not significantly different from each other. The C treatment was significantly different from the other three treatments, with the F-C ($p < 1.1E\text{-}8$), L-C ($p < 3.5E\text{-}9$), and S-C ($p < 2.6E\text{-}9$) treatment pairs all having $p < 0.05$. Though the leachate pH of the L and F samples were not significantly different from the S samples, this could change if the starting soil was more acidic or had less buffering capacity. This could make enhanced weathering of concrete a tool to combat ocean acidification. Taylor et al. (2016) noted this and showed that enhanced weathering over less than one-third of tropical land could have a large impact in counteracting ocean acidification by 2100. With such a wide availability, concrete application need not be limited to tropical areas; intentionally applying concrete to soil in areas where soil water

would end up in the ocean could become a practical method to ameliorate ocean acidification.

A regression analysis was completed to study any relationships between the leachate pHs over time. The results can be seen in Figure 27. The S samples showed little correlation with time, with an R^2 value of 0.19. This is likely because nothing was added to the S samples that should have changed the pH. The C samples show no correlation with an R^2 value of 0.051. Because there was no soil in the C samples, the water quickly passed through the concrete and drained out of the sample. The pH for these samples was likely most related to the path the water took and the exposure time the water had to the concrete. The F samples had a strong correlation with time, with an R^2 value of 0.80, and the L samples also had a moderate correlation with time, with an R^2 value of 0.51. The L and F samples likely had stronger correlations with time compared to the C and S samples because of the presence of both soil and concrete. The L, F, and S treatments had F-tests with $p < 0.05$ indicating a statistically significant correlation between time and leachate pH. The concrete is the material responsible for the increase in pH, and the soil both facilitated and counteracted this change. The soil facilitated the increase in pH because of its ability to retain water and thus increases the exposure time of the water to the concrete. It counteracted the pH increase with organic matter and other materials that helped buffer the pH change. The most notable aspect of these regressions is that it shows the pH values tapering off in the F samples. The high pH in concrete is caused largely in part by sodium and potassium alkalis. These two alkalis were found to leach from the concrete quickly

during the experiment. It is possible that as the concentration of these two compounds decreases in the leachate, the water pH will stabilize.

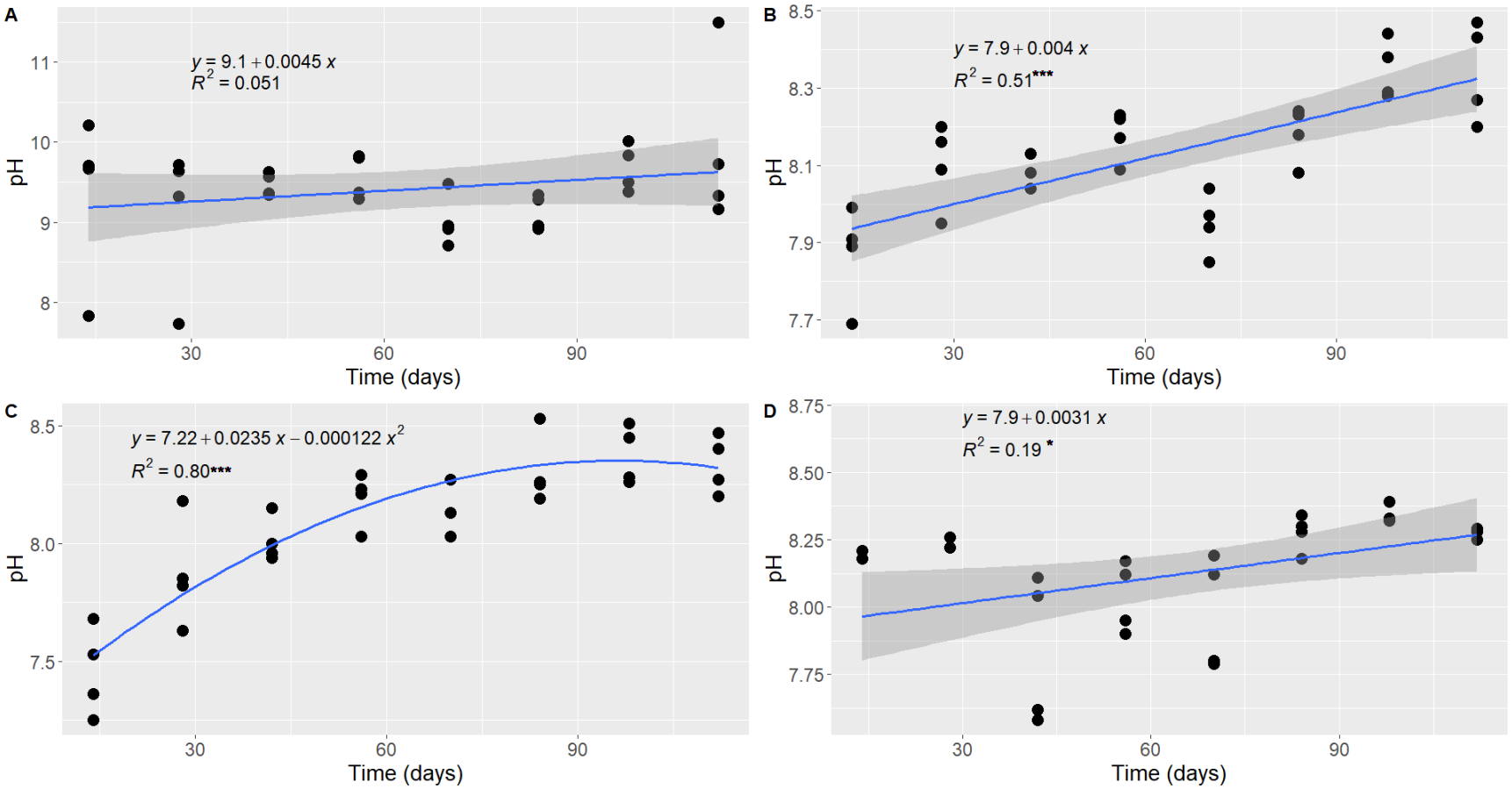

Figure 27 Regression analysis of leachate pH versus time with each graph representing a different treatment. (A) C treatment, (B) L treatment, (C) F treatment, and (D) S treatment. Asterisks signify a $p < 0.05$ for the F-test, indicating a statistically significant correlation between the independent and dependent variable.

pH measurements of soil paste also showed differences between the treatments. The S treatment group had pH values similar to the initial soil below 7 with one outlier, while the L samples and F samples had increased pHs around 7.3 and 8 respectively. The C treatment was not measured as there was no soil present. Figure 28 shows a bar graph with the soil pH values. The F treatment group had a much larger increase in soil pH compared to the L group, however this value may be misleading. Because the concrete fragments added to the F treatment soils were so small, it was not possible to separate them from the soil when taking pH measurements. This meant that the concrete was submerged in water during testing which could have resulted in the same phenomenon seen for the increased pH of the C4 leachate with the blocked drain. Therefore, it is unknown if the pH measured for the F soil samples is accurate.

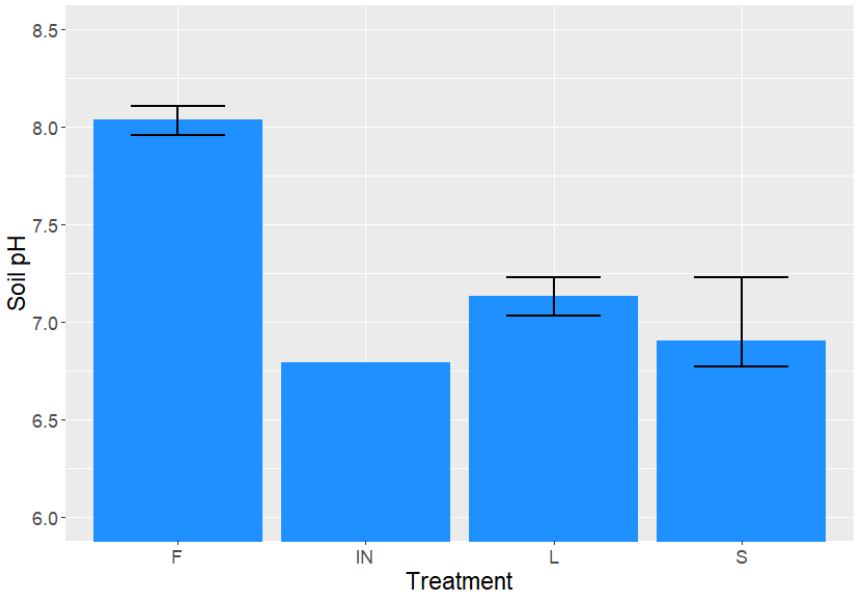

Figure 28 Treatment effects on soil pH with "F" being the samples with small concrete fragments in soil, "IN" being the initial soil samples, "L" being the samples with large concrete fragments in soil, and "S" being the soil only samples.

A Kruskal Wallis rank sum test was used to determine the significance of the soil pH results because the S samples failed the Shapiro-Wilks normality tests. The Kruskal Wallis rank sum test found a $p < 0.01664$, indicating significance of the results. A post-hoc analysis was performed using a Dunn test with a Bonferroni adjustment. Only the comparison between the S and F treatments was found to be significant with a $p < 0.0154$. This result supports the hypothesis that the smaller concrete fragments weathered faster and impacted the soil pH significantly while soil pH in the L samples was not significantly impacted; however, the results from the F sample could have been impacted as mentioned during testing.

These results suggest that concrete could be used as a soil amendment alternative to lime to increase soil pH. Soils that are too acidic can limit plant growth, but they can be remediated by adding lime, an alkaline material, to the soil (Holland et al., 2018). Agricultural lime is typically made from pulverized limestone which is one of the main ingredients in cement and is sometimes used as the coarse aggregate in concrete as it was in this experiment. Recycled concrete could be a sustainable and possibly cheaper alternative to lime because lime would not need to be mined specifically for the purpose of agricultural application.

Sodium

The C, L, and F treatment samples all had sodium concentrations that decreased with time while the S treatment samples stay consistent, shown in Figure 29. The L samples started around 18 ppm and ended around 2 ppm. The F samples started around 30 ppm and

ended around 4 ppm. The S samples were consistently between 1 ppm and 3 ppm. The C treatment concentrations were substantially higher than the other treatments, with the first samples ranging from 30 ppm to 100 ppm and ending around 8 ppm. This can be seen in Figure 29. Because the S samples did not have elevated sodium levels, it was assumed that the concrete was the source of sodium. The known source of sodium in concrete is a sodium alkali, Na_2O, in cement, and it is found in lesser amounts, normally comprising less than 0.5% of the total cement. Seeing that the sodium concentrations approaching 0 ppm is less cause for concern of concrete increasing the sodium concentration of the soil overall.

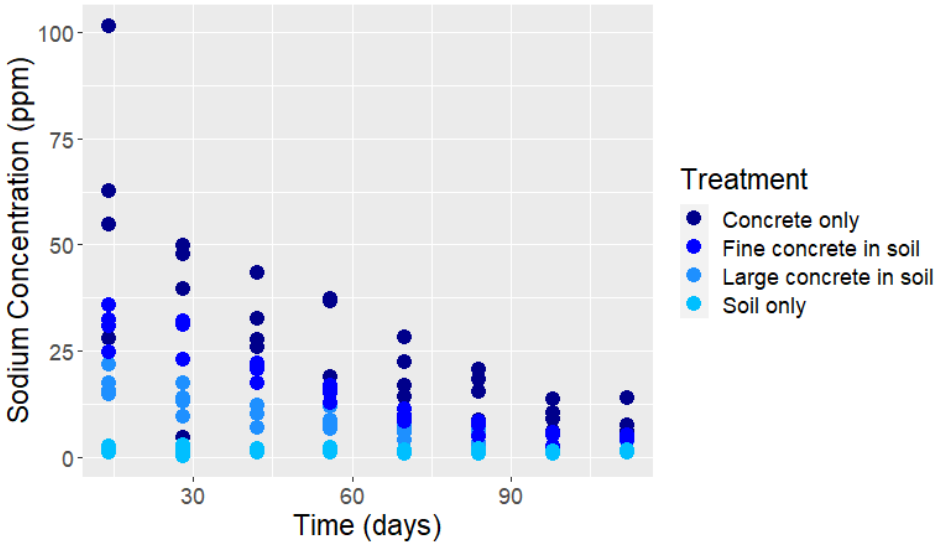

Figure 29 Sodium concentration of leachate over the duration of the experiment

A Kruskal Wallis rank sum test was used to determine the significance of the sodium results because the all samples failed the Shapiro-Wilks normality tests except the F samples. The Kruskal Wallis rank sum test found a $p < 2.2E\text{-}16$, indicating significance of the results. A post-hoc analysis was performed using a Dunn test with a Bonferroni

adjustment. The F treatment was not significantly different than the L or the C treatment. All other treatment pairs, L-C ($p < 0.0093$), S-C ($p < 2E\text{-}16$), S-F ($p < 1.9E\text{-}10$), and S-L (1.7E-5), were significantly different.

A linear regression analysis was completed to study relationships between the leachate sodium concentrations and time. The results can be seen in Figure 30. The S samples showed little correlation with time, with an R^2 value of 0.36. The lack of correlation is not unexpected as the source of sodium is expected to be concrete. The F samples had a very strong correlation with time, with an R^2 value of 0.90. The L samples also had a strong correlation with time, with an R^2 value of 0.81. It is notable that the regression equation for the F samples is almost twice the equation of the L samples, with F samples having a slope of -0.3 and L samples having a slope of -0.15, meaning that the F samples are losing sodium at twice the rate of the L samples. This is due to the smaller fragment sizes in the F samples which react more quickly. The C samples showed a moderate correlation with an R^2 value of 0.56. The L and C samples contain the same sized concrete fragments, and the C samples contain on average about 8.5 times more concrete by weight. Because of this, it was expected to see sodium concentrations in the L samples that were 8.5 times less than the sodium concentrations of the C samples. However, the slope of the regression equation for the C samples is only three times larger than the slope of the L sample regression equation. Sodium from the L samples is also likely getting captured on the soil CEC, meaning the difference in sodium concentrations between the L and C samples is even less than shown from the regression. This is likely due to an increased weathering rate of the concrete in the L samples because of the soil. All four

treatments had F-tests with $p < 0.05$ indicating a statistically significant correlation between time and the sodium concentration in the leachate.

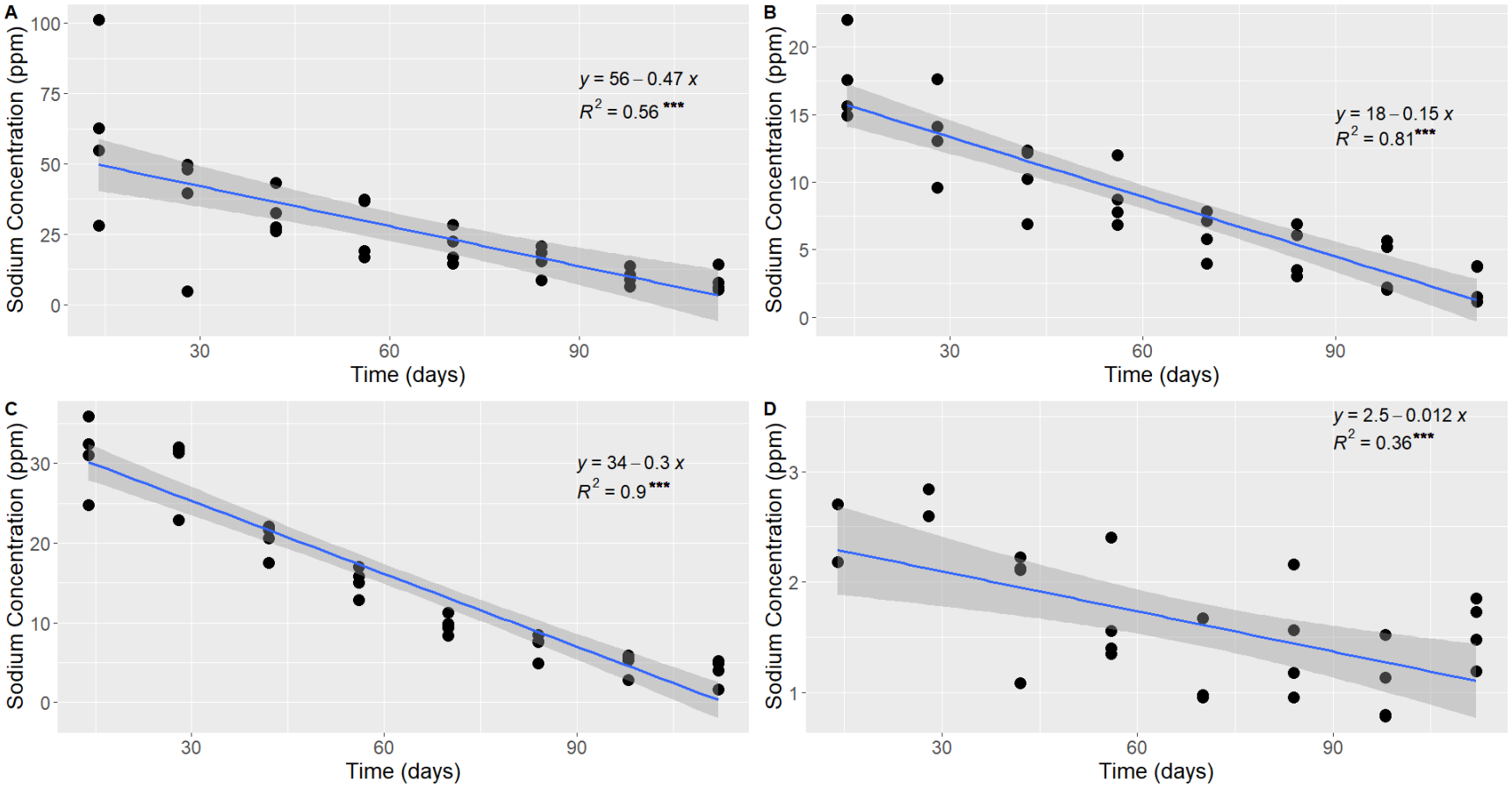

Figure 30 Regression analysis of leachate sodium concentrations versus time with each graph representing a different treatment. (A) C treatment, (B) L treatment, (C) F treatment, and (D) S treatment. Asterisks signify a $p < 0.05$ for the F-test, indicating a statistically significant correlation between the independent and dependent variable.

It was believed that sodium was being captured in the soil due to the CEC of the soil, so SAR testing was conducted to test this. Soils with SAR values greater than 13 are considered sodic soils; these soils have high concentrations of sodium relative to magnesium and calcium at the cation exchange sites. Sodic soils have poor soil structure due to the dispersion of aggregates caused by excess sodium levels and can lead to poor plant growth. Normally SAR is expected to relate to pH, however Figure 31 shows that not to be true for these samples. Similarly, no correlations were found between SAR values and the different treatments, meaning that adding concrete to soil does not correlate to an increase in the SAR of a soil. This is likely because as the sodium concentrations increased from the concrete weathering, the calcium concentrations also increased; magnesium concentrations were not found to differ greatly between the S, L, and F treatments, therefore not impacting the SAR values. Sodium leaching is not viewed as a concern from concrete weathering in soil because the concentration of sodium in concrete is so small, and because any increase in the sodium concentration will be offset by an increase in the calcium concentration.

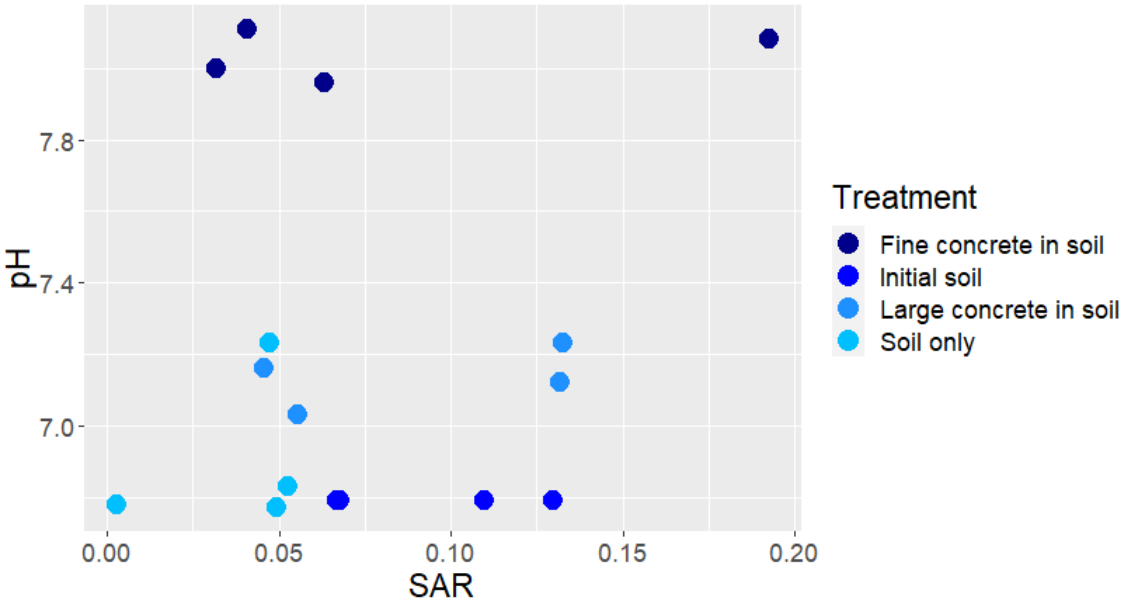

Figure 31 Soil SAR vs. soil pH

The sodium concentrations in the C, L, and F samples all decreased dramatically in a brief period of time, suggesting that sodium oxides in concrete weather readily. Concrete also contains potassium oxides and similar trends were observed in the leachate potassium concentrations; Figure 32 shows an almost perfect linear relationship between the amount of potassium and sodium in the C leachate. Regression was only done on the C treatment because sodium and potassium in the L and F samples were thought to be caught on the CEC and would not show the true relationship. The F-test had a $p < 0.05$ indicating a statistically significant correlation between potassium and the sodium concentrations in the leachate. This regression confirms that potassium oxides in concrete also readily weather.

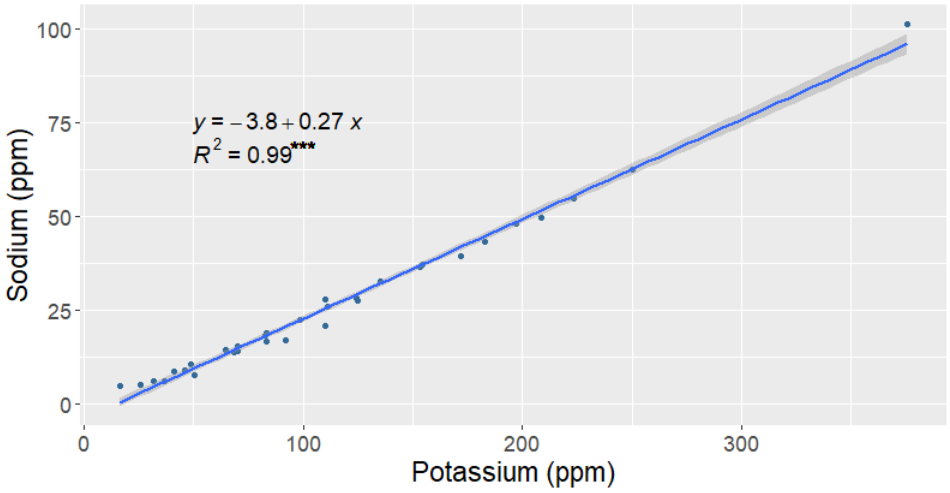

Figure 32 Potassium leachate concentration versus sodium leachate concentration of C samples. Asterisks signify a $p < 0.05$ for the F-test, indicating a statistically significant correlation between the independent and dependent variable.

Because of the large amount of calcium concrete loses during carbonation, concrete has potential as a sodic soil amendment. The order in which ions on the soil CEC are replaced depends on an ion's valence and dehydrated radius; this replacement order is called the lyotropic series (Bohn et al., 2001). Equation 13 shows part of the Lyotropic series, with the most strongly bonded ions on the left and the most easily lost ions on the right.

Equation 13 Lyotropic series

$$Ba^{2+} \approx Sr^{2+} > Ca^{2+} > Mg^{2+} \approx Cs^{+} > Rb^{+} > NH_4^{+} \approx K^{+} > Na^{+} \approx Li^{+}$$

Per the lyotropic series, sodium is replaced on the soil CEC by calcium. Knowing this, concrete could be used as a material to remediate sodic soils which have excess sodium.

Gypsum is one amendment used currently to remediate sodic soils, but recycled concrete could be an alternative calcium source to replace sodium in these soils.

Aggregate stability

Table 11 shows the results from the ANOVA statistical testing used to analyze differences in the aggregate stability. Minor measurement errors resulted in water stable aggregate (WSA) values greater than 100%, therefore these results were not analyzed. No significant differences were found in soil mean weight diameter (MWD) and geometric mean diameter (GMD) between the treatments, but significant differences were found between soil moisture contents.

Table 11 Aggregate stability results with "L" being the samples with large concrete fragments in soil, "F" being the samples with small concrete fragments in soil, and "S" being the soil only samples.

Treatment	Moisture content*		%WSA		MWD** (mm)		GMD** (mm)	
	Mean	Std Dev	Mean	Std Dev	Mean	Std Dev	Mean	Std Dev
L	16%	1.5%	100	1.0	5.75	0.26	2.07	0.08
F	16%	2.4%	101	1.3	6.17	0.13	2.19	0.06
S	10%	1.2%	97	1.6	5.69	0.53	1.96	0.18

*ANOVA $p < 0.00236$
** ANOVA not significant
*** ANOVA not significant

The difference in moisture content could be because of water trapped in the pore spaces in the concrete fragments, however this likely is not the reason since the F samples would be expected to have the highest moisture contents. Another more likely reason for the difference in moisture content is that the L and F samples had higher porosities and were

able to store more water. S samples were placed into the soil columns as intact soil cores, but the L and F samples were mixed with concrete and then put into the columns with a smaller overall density. This would leave more pore space in the soil available for water to be stored. Overall, the aggregate stability of the soil was not impacted by the addition of concrete.

Microorganisms

Changes in soil bacteria, fungi, and protozoa were tested to understand what impacts adding concrete to soil had on the microbial community. Increases in microbial populations were interpreted as being synonymous with beneficial soil conditions while decreases in microbial populations were interpreted as being synonymous with detrimental soil conditions. Figure 33 shows the concentrations of the microbial communities in each sample. The concentrations of all three types of microorganisms were greater in the S samples than the concentrations in the initial soil samples. This trend could be because the S samples were consistently watered during the experiment and microbes generally thrive in moist environments. The microbial communities in the L samples were larger than in the initial soil samples, but not as large as the S samples. The microbial communities in the F samples were considerably smaller than the other samples.

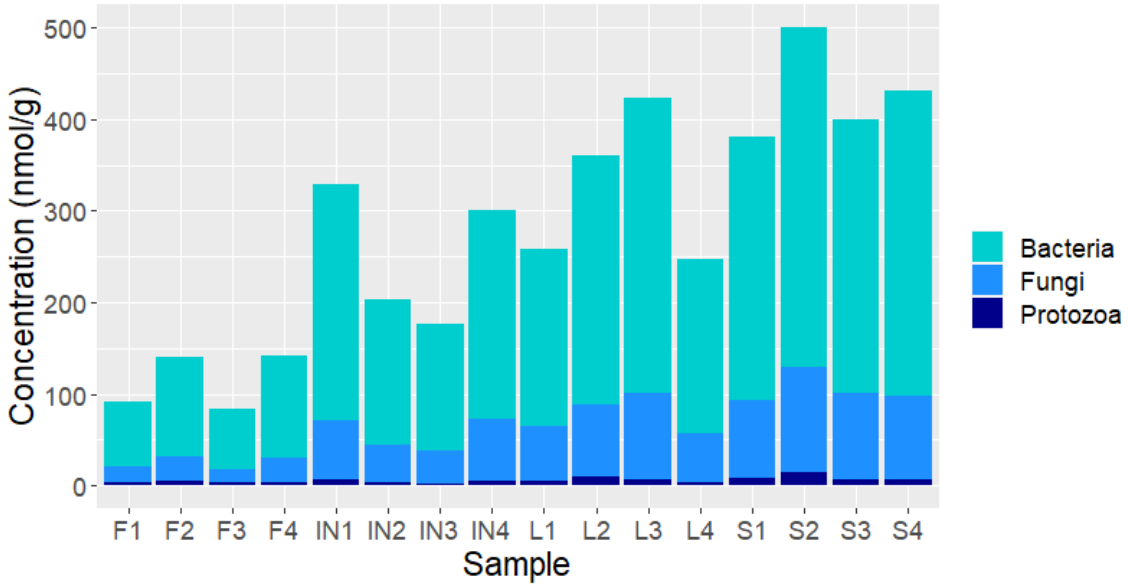

Figure 33 Concentration of soil bacteria, fungi, and protozoa with "F" being the samples with small concrete fragments in soil, "IN" being the initial soil samples, "L" being the samples with large concrete fragments in soil, and "S" being the soil only samples.

ANOVA statistical testing was used to analyze differences in the soil microbial communities. Shapiro-Wilks normality tests were completed first to confirm normality of the samples, but the Protozoa data did not pass the normality test and was instead analyzed with a Kruskal Wallis rank sum test. Significant differences were found in the protozoa ($p < 0.02082$), fungi ($p < 7.95E-05$), and bacteria ($p < 0.00153$) communities. To further analyze the data, a post hoc analysis was done. Tukey's range test was completed on the fungi and bacteria to determine which treatments were significantly different. This test could not be completed on the protozoa because the data was not normal so instead a Dunn test with a Bonferroni adjustment was performed. The results of this test are shown in Figure 34.

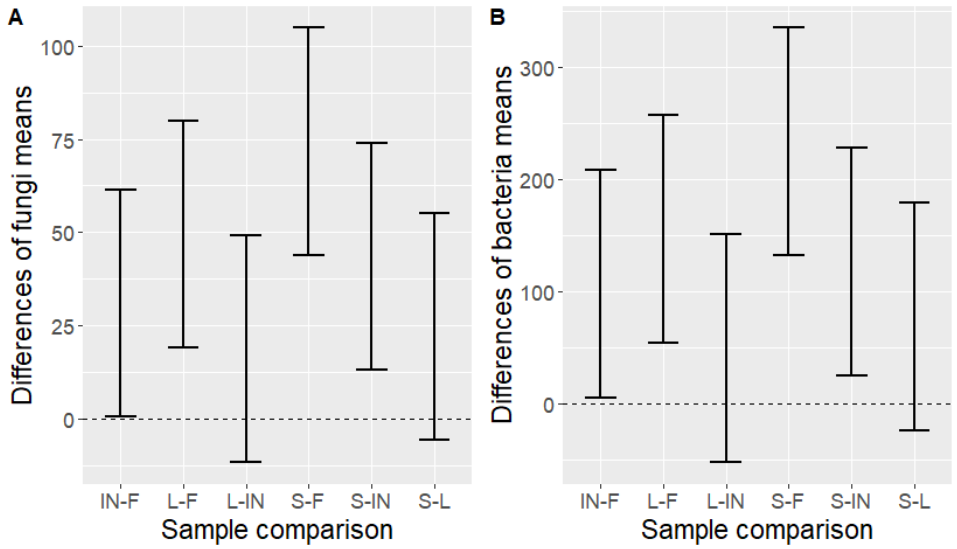

Figure 34 Tukey range test plots with 95% confidence level for fungi (A) and bacteria (B) with "L" being the samples with large concrete fragments in soil, "F" being the samples with small concrete fragments in soil, , "IN" being the initial soil samples, and "S" being the soil only samples. Ranges that include 0 are considered insignificant.

Significant differences in protozoa were only found between the S and F treatments ($p < 0.0451$). Significant differences in fungi were found between the IN-F ($p < 0.0459$), L-F ($p < 0.00196$), S-F (($p < 0.000051$), and S-IN ($p < 0.00539$) treatments. Significant differences in bacteria were found between the IN-F ($p < 0.0386$), L-F (0.00317), S-F ($p < 0.000093$), and S-IN ($p < 0.0136$) treatments. Fungi prefer acidic conditions which was likely the cause of decline in the fungi community in the F samples (Rousk et al., 2009). Similar trends were seen for the bacterial community. This can be interpreted to mean that the F treatment was detrimental to soil microorganisms, but the L treatment was not because it was not significantly different from either the S or IN treatments. This shows that concrete in soil can harm microorganisms which would damage the overall soil health.

However, managed correctly, the L treatment shows that it is possible to add concrete to soil without harming soil microbes.

Nitrogen

Nitrogen concentrations found in the leachate are shown in Figure 35. From the anion analysis it was determined that the nitrogen in the samples was in the form of nitrate. Nitrate was found in higher concentrations in the L and F treatment leachate which was unexpected. Nitrate concentrations in the L samples ranged from 3 ppm to 40 ppm while concentrations in the F samples ranged from 1 ppm to 70 ppm. Nitrate concentrations in the C samples stayed below 0.2 ppm. In the S samples, concentrations stayed below 6 ppm with the exception of S2 for weeks 3 through 6 which saw nitrate concentrations ranging from 19 ppm to 37 ppm. There are no known sources of nitrate in concrete, and the C samples contained negligible amounts of nitrate, so it was assumed the nitrate was coming from the soil.

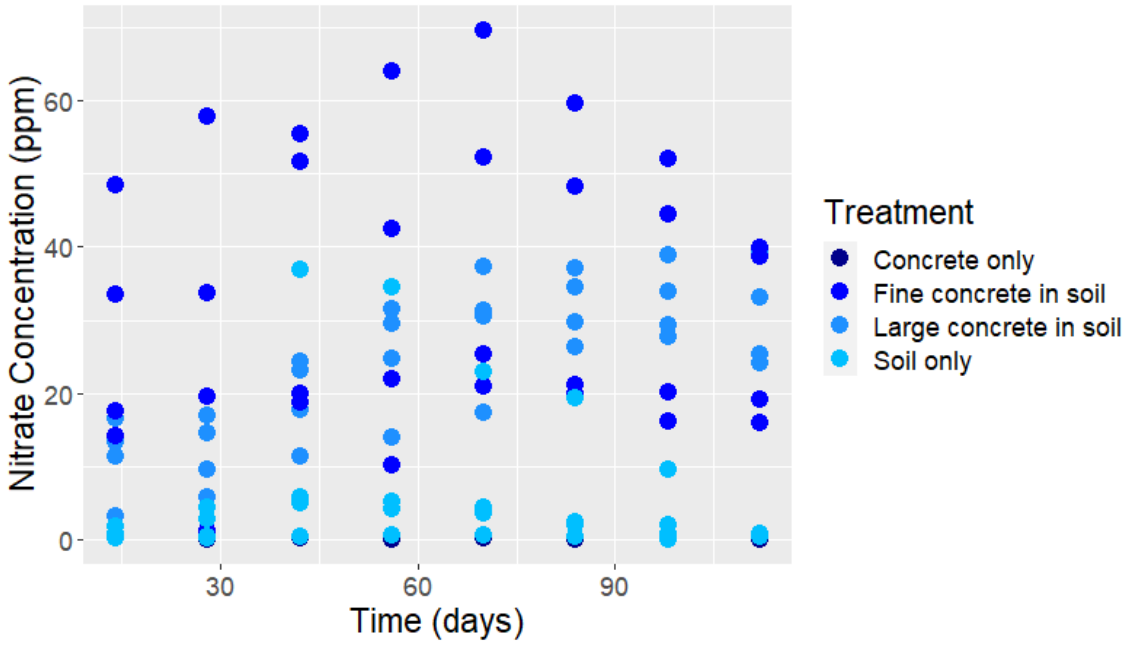

Figure 35 Nitrate concentration of leachate over the duration of the experiment

To confirm that soil was the source of the nitrate, soil samples were analyzed to see if the leachate that higher concentrations of nitrate had smaller concentrations of nitrogen in the soil, meaning the nitrate had been lost from the soil. These results, shown in Figure 36, confirm this theory. Nitrate in the soil likely was sourced from organic matter which solubilized and leached out when concrete was added to soil and increased the pH.

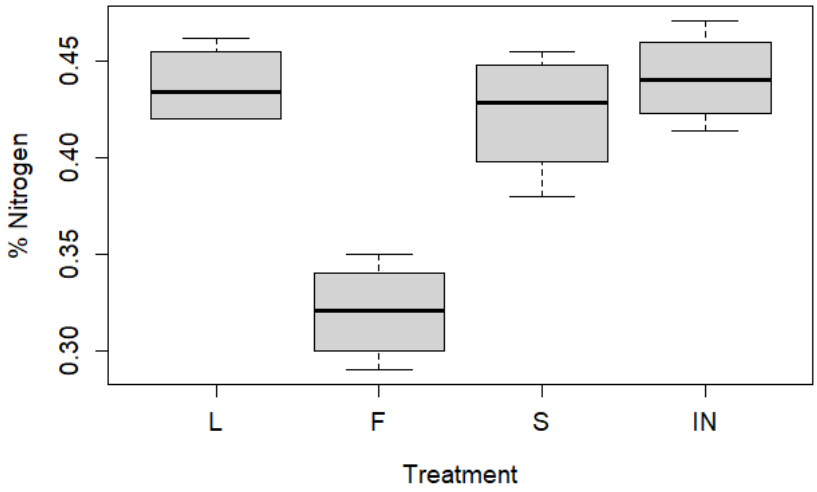

Figure 36 Soil sample nitrogen results with "L" being the samples with large concrete fragments in soil, "F" being the samples with small concrete fragments in soil, "S" being the soil only samples, and "IN" being the initial soil samples.

ANOVA statistical testing was used to determine the significance of the nitrate results. Shapiro-Wilks normality tests were completed first to confirm normality of the samples. The F and S samples did not pass the normality test, so instead a Kruskal Wallis rank sum test was done. The Kruskal Wallis rank sum test found a $p < 2.2E\text{-}16$, confirming significance of the results. A post-hoc analysis was performed using a Dunn test with a Bonferroni adjustment. Significant differences were seen between the F-C ($p < 2E\text{-}16$), L-C ($p < 1.03E\text{-}13$), S-C ($p < 0.00135$), S-F ($p < 2.9e\text{-}6$), and S-L ($p < 0.0041$) treatment pairs which includes every treatment pair except L-F.

Total soil carbon was measured alongside soil nitrogen. The ratio of carbon to nitrogen (C:N ratio) in soil is vital in soil because it impacts organic matter decomposition rates and turnover rates of nitrogen (Janssen, 1996). Figure 37 shows the total carbon content which includes both organic and inorganic carbon in the samples. The concrete

fragments in the F samples were too small to be sieved out and are likely the cause of the increased carbon content, so the change in organic carbon content is unknown. Because the carbon measured was total carbon rather than organic carbon, a C:N ratio calculation is not possible. It is notable that the carbon content of the L sample is higher than that of the S and IN treatments which could be a measurement of carbonates formed because of concrete carbonation.

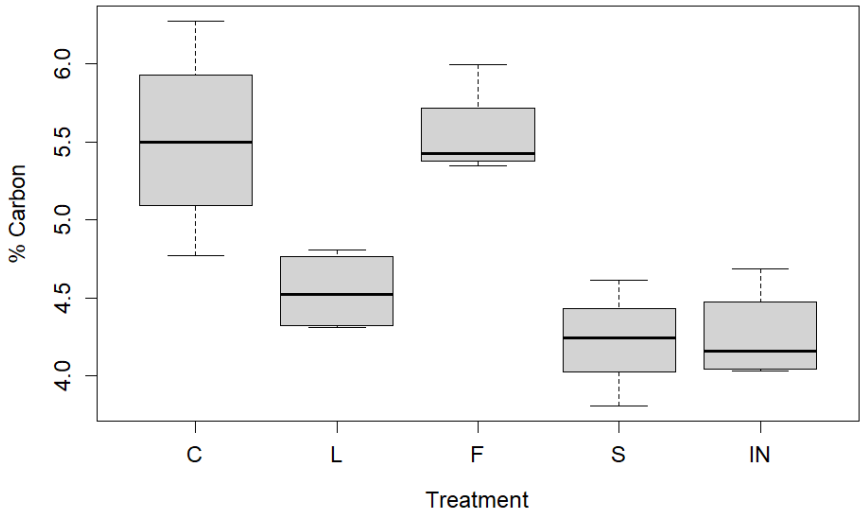

Figure 37 Carbon soil sample results with "C" being the concrete only samples, "L" being the samples with large concrete fragments in soil, "F" being the samples with small concrete fragments in soil, "S" being the soil only samples, and "IN" being the initial soil samples.

A linear regression analysis was completed to study relationships between the leachate nitrate concentrations and time. The results can be seen in Figure 38. The C and L samples showed a moderate correlation with time, with R^2 values of 0.5 and 0.6 respectively, and had F-tests with $p < .05$ indicating a statistically significant correlation between time and nitrate concentration in the leachate. However, because the C samples had so little nitrate

the correlation is not meaningful. The F and S samples showed no correlation with time, with R^2 values of 0.0029 and 0.028 respectively. The lack of correlation in the S samples is not unexpected because there was nothing added to the S samples that would have caused a change in the nitrate concentrations. The slower weathering rate of the concrete in the L samples due to the larger fragment sizes may be the cause of the more linear relationship between time and nitrate concentration.

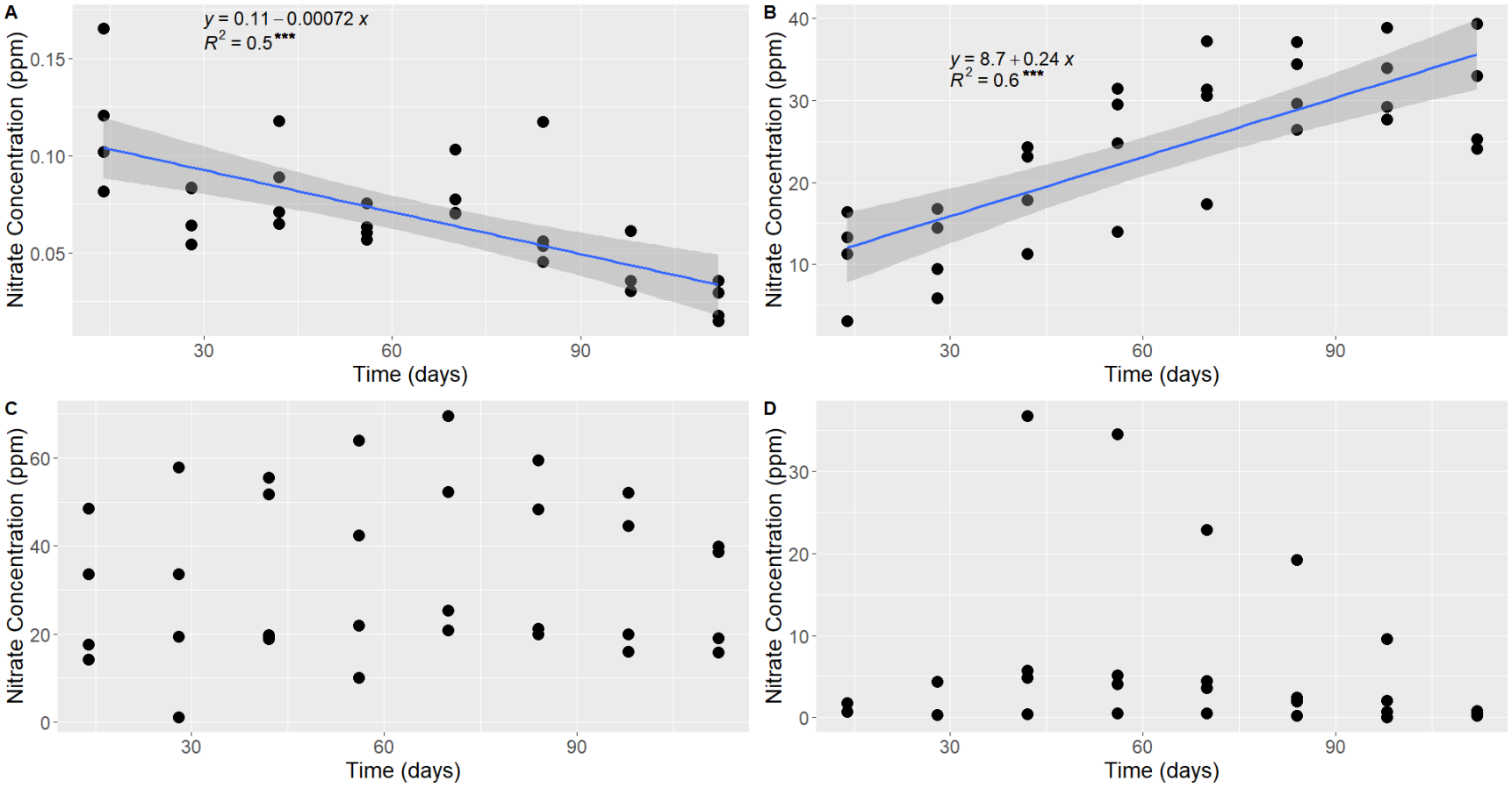

Figure 38 Regression analysis of leachate nitrate concentrations versus time with each graph representing a different treatment. (A) C treatment, (B) L treatment, (C) F treatment, and (D) S treatment. Asterisks signify a $p < 0.05$ for the F-test, indicating a statistically significant correlation between the independent and dependent variable.

The relationship between leachate pH and leached nitrate was investigated, shown in Figure 39. Nitrate concentrations appeared to generally increase until week 10 after which concentrations began to decrease which is close to the time when leachate pHs began to level off. No clear trend was found between leachate pH and nitrate concentration.

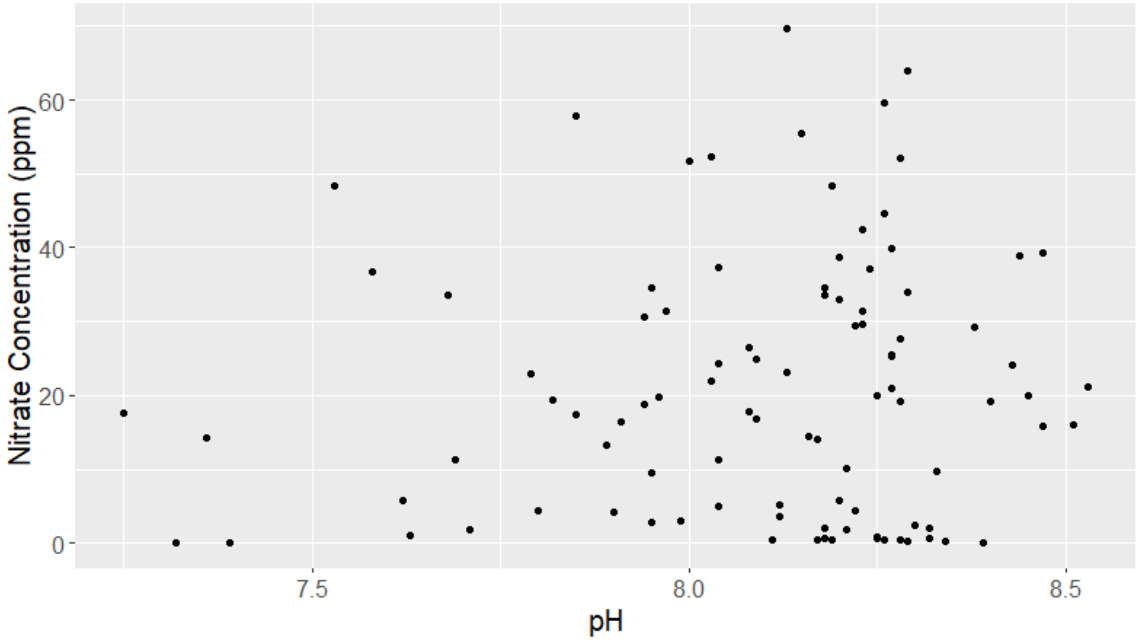

Figure 39 Nitrate vs. pH of leachate for the L, F, and S treatment samples

Figure 40 shows the relationship between soil pH and cumulative nitrate from the leachate over the course of the experiment. These variables have a clearer relationship compared to the pH values of the leachate and nitrate concentrations. The model F-test had a $p < 0.05$ indicating a statistically significant correlation between pH and cumulative nitrate concentration in the leachate.

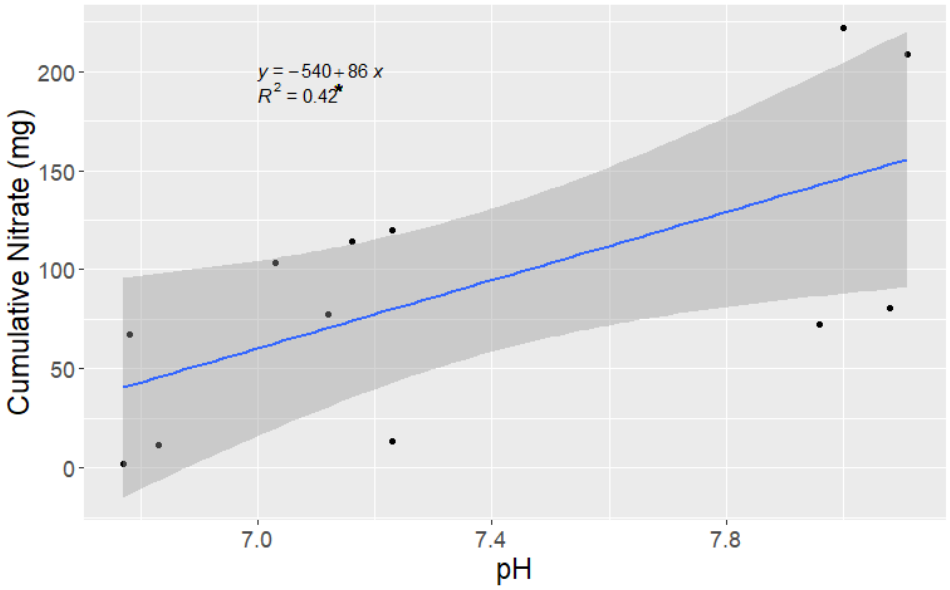

Figure 40 Final soil pH versus cumulative leached nitrate. Asterisks signify a $p < 0.05$ for the F-test, indicating a statistically significant correlation between the independent and dependent variable.

The release of nitrate could be a benefit of adding concrete as a soil amendment. Less nitrogen in the soil could lead to slower decomposition rates and longer organic carbon turnover times. Microorganisms require nitrogen as an energy source to decompose organic matter, so organic matter that has smaller amounts of nitrogen would take longer to decompose. On the other hand, concrete causing a release of nitrate from soil could be detrimental to nature and human health. Aquatic plants and algae can grow too quickly when water bodies contain high concentrations of nitrate. This causes the formation of harmful algal blooms which can starve other marine life of oxygen and cause hypoxia like what is seen in Lake Erie and the Gulf of Mexico (Kharbush et al., 2023; Rabalais and Turner, 2019). Too much nitrate in drinking water can cause infant methemoglobinemia, also called “blue baby syndrome”, leaving babies unable to get enough oxygen in their blood (Knobeloch et al., 2000). The United States Environmental Protection Agency limits

nitrate in drinking water to 10 ppm, which is lower than the nitrate concentrations of both the L and F treatment samples (US EPA, 2023). While this water could be treated at a water treatment plant, people that rely on groundwater as a drinking water source would be at risk. Nitrate leaching caused by the addition of concrete to soil has both positive and negative potential effects. Further studies are needed to better understand the extent of nitrate leaching and how it would change under real-world conditions.

Conclusions

- The leachate pH of the mixed concrete and soil samples were not significantly different from the soil only samples, and the F treatment soils were significantly different from the L and S treatment soils. This could make concrete a useful lime substitute or a solution to ocean acidification.
- Sodium is quickly weathered from concrete, both in the presence and absence of soil. Because of the dual release of calcium, soil SAR is not negatively impacted by the addition of concrete, and concrete could be used as a tool to amend sodic soils.
- Aggregate stability is not impacted by the addition of concrete.
- Fungi, protozoa, and bacteria communities were all negatively impacted in the F samples but were not impacted in the L samples, showing that concrete could be added to soil that would not harm microbial communities.
- Nitrate was significantly elevated in both the L and F samples compared to the S and C samples. This nitrate was likely from organic matter that was solubilized

due to a change in pH. The increase in leachate nitrate could cause harm to nature by aiding the growth of harmful algal blooms and to humans in ground water used as drinking water.

Chapter 6: Summary and Conclusions

The objectives of this research were to conduct a laboratory experiment and investigate the carbonation of concrete within soil as a viable option to sequester atmospheric carbon, analyze how the carbonation of concrete changes with fragment size, and understand the environmental impacts of adding concrete to soil. It was hypothesized that concrete in soil would experience carbonation faster than concrete alone. It was also hypothesized that soil samples with smaller concrete fragments would experience carbonation at a faster rate compared to the larger fragments because of the increased reactivity from increased surface area.

The results from this study show that concrete has potential as an enhanced weathering material in soil to sequester large amounts of carbon dioxide from the atmosphere. Significant differences between the C samples and the L and F samples showed that soil facilitates faster concrete weathering rates. This study found that putting 120-150 g of concrete in soil sequestered 0.15-1.8 g of CO_2. Modeling the data, it is predicted that for every 1 m^2 surface area of concrete added to soil, 2.1 g of atmospheric carbon is sequestered annually. Significant differences between the L and F samples also show that the smaller concrete fragments weather faster than larger concrete fragments. Although the smaller fragments weather faster and sequester more carbon in the short term, it is thought that the

larger fragments would continue weathering and eventually sequester similar amounts of CO_2.

Adding concrete to soil was found to impact soil and water quality. Concrete in soil was found to increase the soil pH of the F samples but did not impact leachate pH. In some cases, this could make concrete a useful lime substitute or a solution to ocean acidification. Sodium is quickly weathered from concrete, both in the presence and absence of soil. Because of the dual release of calcium, soil SAR was not significantly different in the L and F samples compared to the S samples, and concrete could be used as a tool to amend sodic soils. Aggregate stability was not found to be impacted by the addition of concrete. The microbial community was affected by the presence of concrete, with the fungi, protozoa, and bacteria communities all significantly smaller in the F samples. However, these communities were not impacted in the L samples, proving that concrete can be added to soil without harming microbes. Increased nitrate levels were found in the L and F samples. This increase in leachate nitrate could cause harm to nature and humans by aiding the growth of harmful algal blooms and impacting ground water used as drinking water.

The different constituents measured during the experiment relate to each other in different ways. Figure 41 is a correlation matrix showing the general correlation between measured components in F and L samples, the two mixed treatments.

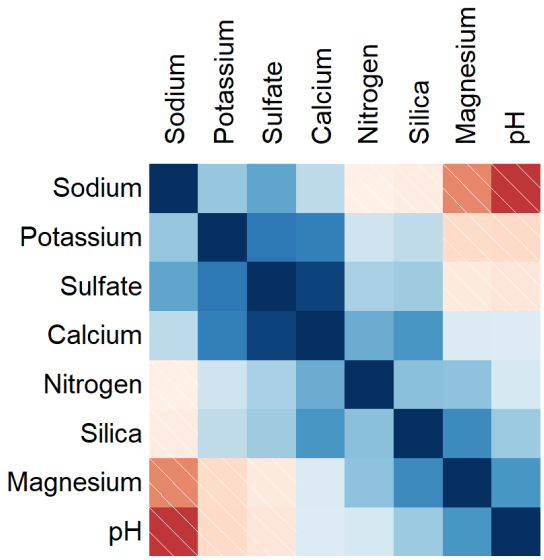

Figure 41 Correlation matrix showing the general correlation between measured components in F and L samples. Dark red indicates a more negative correlation while dark blue indicates a more positive correlation.

Future studies should focus on maximizing the weathering and carbon sequestration potential of concrete while minimizing environmental impacts. The two most important environmental impacts to monitor per this study are the release of nitrate in leachate and the health of the microbial community. Differences between the L and F samples give evidence that these impacts can be managed by altering the fragment size of the concrete. Other additives to soil in conjunction with concrete may be able to reduce environmental damage. Future studies should also analyze how changes in concrete composition affect CO_2 sequestration rates and environmental effects.

Bibliography

Abbaspour, Aiyoub, and Burak F. Tanyu. “CO 2 Sequestration by Carbonation Processes of Rubblized Concrete at Standard Conditions and the Related Mineral Stability Diagrams.” ACS Sustainable Chemistry & Engineering, vol. 8, no. 17, May 2020, pp. 6647–56. DOI.org (Crossref), https://doi.org/10.1021/acssuschemeng.9b07690.

Andrade, Carmen, and Miguel Ángel Sanjuán. “Carbon Dioxide Uptake by Pure Portland and Blended Cement Pastes.” Developments in the Built Environment, vol. 8, Sept. 2021, p. 100063. ScienceDirect, https://doi.org/10.1016/j.dibe.2021.100063.

Andrew, Robbie M. Global CO2 Emissions from Cement Production, 1928–2017. 2018, p. 27.

Beerling, David J., et al. “Potential for Large-Scale CO2 Removal via Enhanced Rock Weathering with Croplands.” Nature, vol. 583, no. 7815, 7815, July 2020, pp. 242–48. www-nature-com.proxy.lib.ohio-state.edu, https://doi.org/10.1038/s41586-020-2448-9.

Behnood, Ali, et al. “Methods for Measuring PH in Concrete: A Review.” Construction and Building Materials, vol. 105, Feb. 2016, pp. 176–88. ScienceDirect, https://doi.org/10.1016/j.conbuildmat.2015.12.032.

Ben Ghacham, Alia, et al. “CO2 Sequestration Using Waste Concrete and Anorthosite Tailings by Direct Mineral Carbonation in Gas–Solid–Liquid and Gas–Solid Routes.” Journal of Environmental Management, vol. 163, Nov. 2015, pp. 70–77. DOI.org (Crossref), https://doi.org/10.1016/j.jenvman.2015.08.005.

Berner, Robert A. “Weathering, Plants, and the Long-Term Carbon Cycle.” Geochimica et Cosmochimica Acta, vol. 56, no. 8, Aug. 1992, pp. 3225–31. ScienceDirect, https://doi.org/10.1016/0016-7037(92)90300-8.

Bertos Fernández, M., et al. “A Review of Accelerated Carbonation Technology in the Treatment of Cement-Based Materials and Sequestration of CO2.” Journal of Hazardous Materials, vol. 112, no. 3, Aug. 2004, pp. 193–205. ScienceDirect, https://doi.org/10.1016/j.jhazmat.2004.04.019.

Biernacki, Joseph J., et al. “Cements in the 21st Century: Challenges, Perspectives, and Opportunities.” Journal of the American Ceramic Society. American Ceramic Society, vol. 100, no. 7, July 2017, pp. 2746–73. PubMed Central, https://doi.org/10.1111/jace.14948.

Blake, G. R., and K. H. Hartge. “Bulk Density.” Methods of Soil Analysis Part 1, Second, American Society of Agronomy, Inc. and Soil Science Society of America, Inc., 1986, pp. 364–67.

Bohn, Hinrich, et al. “Electrostatic Cation Retengion (Cation Exchange).” Soil Chemistry, 3rd ed., John Wiley and Sons, Inc, 2001, pp. 207–214.

Brady, Patrick V., and John V. Walther. “Controls on Silicate Dissolution Rates in Neutral and Basic PH Solutions at 25°C.” Geochimica et Cosmochimica Acta, vol. 53, no. 11, Nov. 1989, pp. 2823–30. ScienceDirect, https://doi.org/10.1016/0016-7037(89)90160-9.

Carlson, C. A., et al. “Carbon Cycle.” Encyclopedia of Ocean Sciences (Second Edition), edited by John H. Steele, Academic Press, 2001, pp. 477–86. ScienceDirect, https://doi.org/10.1016/B978-012374473-9.00272-1.

Castro, P., et al. “Influence of Marine Micro-Climates on Carbonation of Reinforced Concrete Buildings.” Cement and Concrete Research, vol. 30, no. 10, Oct. 2000, pp. 1565–71. ScienceDirect, https://doi.org/10.1016/S0008-8846(00)00344-6.

Charlson, R. J., and H. Rodhe. “Factors Controlling the Acidity of Natural Rainwater.” Nature, vol. 295, no. 5851, 5851, Feb. 1982, pp. 683–85. www-nature-com.proxy.lib.ohio-state.edu, https://doi.org/10.1038/295683a0.

Cheng, Yongchun, et al. “Quantitative Analysis of Concrete Property under Effects of Crack, Freeze-Thaw and Carbonation.” Construction & Building Materials, vol. 129, Dec. 2016, pp. 106–15. a9h.

Chitte, Ketan G., and J. S. Narkhede. “Carbonation of Concrete and Ways of Anticipation.” Paintindia, vol. 66, no. 12, Dec. 2016, pp. 51–56. bth.

Choi, Byoung-Young, et al. “Alteration Processes of Cement Induced by CO (Sub 2) - Saturated Water and Its Effect on Physical Properties; Experimental and Geochemical Modeling Study.” Chemie Der Erde, vol. 76, no. 4, Dec. 2016, pp. 597–604. guh, EBSCOhost, https://doi.org/10.1016/j.chemer.2016.10.001.

Conyers, M. K., et al. “Long-Term Benefits of Limestone Applications to Soil Properties and to Cereal Crop Yields in Southern and Central New South Wales.” Australian

Journal of Experimental Agriculture, vol. 43, no. 1, 2003, pp. 71–78. www-publish-csiro-au.proxy.lib.ohio-state.edu, https://doi.org/10.1071/ea01121.

Dayaram, Kiran, et al. UPTAKE OF CARBON DIOXIDE IN NEW ZEALAND CONCRETE : PRELIMINARY FINDINGS. 2008.

Demars, S., and G. Benoit. "Leaching of ANC and Chromium from Concrete: Effect of Aging Simulated by Sample Carbonation." Water, Air & Soil Pollution, vol. 230, no. 7, July 2019, p. N.PAG-N.PAG. fsr.

Deschner, Florian, et al. "Hydration of Portland Cement with High Replacement by Siliceous Fly Ash." Cement and Concrete Research, vol. 42, no. 10, Oct. 2012, pp. 1389–400. ScienceDirect, https://doi.org/10.1016/j.cemconres.2012.06.009.

Dietzel, M., and J. HOEFSt. "Chemical and 13C/12C-and LSo/160-Isotope Evolution of Alkaline Drainage Waters and the Precipitation of Calcite." Applied Geochemistr, vol. 7, Mar. 1992, pp. 177–84.

Drever, James I. "The Effect of Land Plants on Weathering Rates of Silicate Minerals." Geochimica et Cosmochimica Acta, vol. 58, no. 10, May 1994, pp. 2325–32. ScienceDirect, https://doi.org/10.1016/0016-7037(94)90013-2.

Dunsmore, H. E. "A Geological Perspective on Global Warming and the Possibility of Carbon Dioxide Removal as Calcium Carbonate Mineral." Energy Conversion and Management, vol. 33, no. 5, May 1992, pp. 565–72. ScienceDirect, https://doi.org/10.1016/0196-8904(92)90057-4.

Ehleringer, J. R., et al. A History of Atmospheric CO_2 and Its Effects on Plants, Animals, and Ecosystems. Springer, 2005.

Ekolu, S. O. "A Review on Effects of Curing, Sheltering, and CO2 Concentration upon Natural Carbonation of Concrete." Construction and Building Materials, vol. 127, Nov. 2016, pp. 306–20. DOI.org (Crossref), https://doi.org/10.1016/j.conbuildmat.2016.09.056.

Galan, Isabel, et al. "Sequestration of CO 2 by Concrete Carbonation." Environmental Science & Technology, vol. 44, no. 8, Apr. 2010, pp. 3181–86. DOI.org (Crossref), https://doi.org/10.1021/es903581d.

Gardner, Walter H. "Water Content." Methods of Soil Analysis Part 1, Second, American Society of Agronomy, Inc. and Soil Science Society of America, Inc., 1986, pp. 493–507.

Gasser, T., et al. “Negative Emissions Physically Needed to Keep Global Warming below 2 °C.” Nature Communications, vol. 6, no. 1, 1, Aug. 2015, p. 7958. www-nature-com.proxy.lib.ohio-state.edu, https://doi.org/10.1038/ncomms8958.

Gibson, Michael A., and Don W. Byerly. “Lessons from Limestone; How to Teach All Sciences with Limestone.” Field Guide (Geological Society of America), vol. 50, 2018, pp. 23–47. geh, EBSCOhost, https://doi.org/10.1130/2018.0050(02).

Guo, Rui, et al. “Global CO2 Uptake by Cement from 1930 to 2019.” Earth System Science Data, vol. 13, no. 4, Oct. 2021, pp. 1791–805. a9h.

Hangx, Suzanne J. T., and Christopher J. Spiers. “Coastal Spreading of Olivine to Control Atmospheric CO2 Concentrations: A Critical Analysis of Viability.” International Journal of Greenhouse Gas Control, vol. 3, no. 6, Dec. 2009, pp. 757–67. ScienceDirect, https://doi.org/10.1016/j.ijggc.2009.07.001.

Haque, Fatima, et al. “Optimizing Inorganic Carbon Sequestration and Crop Yield With Wollastonite Soil Amendment in a Microplot Study.” Frontiers in Plant Science, vol. 11, 2020. Frontiers, https://www.frontiersin.org/article/10.3389/fpls.2020.01012.

Hartmann, Jens, et al. “Enhanced Chemical Weathering as a Geoengineering Strategy to Reduce Atmospheric Carbon Dioxide, Supply Nutrients, and Mitigate Ocean Acidification.” Reviews of Geophysics, vol. 51, no. 2, 2013, pp. 113–49. Wiley Online Library, https://doi.org/10.1002/rog.20004.

Holland, J. E., et al. “Liming Impacts on Soils, Crops and Biodiversity in the UK: A Review.” Science of The Total Environment, vol. 610–611, Jan. 2018, pp. 316–32. ScienceDirect, https://doi.org/10.1016/j.scitotenv.2017.08.020.

Holmén, Kim. “11 The Global Carbon Cycle.” International Geophysics, edited by Samuel S. Butcher et al., vol. 50, Academic Press, 1992, pp. 239–62, https://doi.org/10.1016/S0074-6142(08)62694-7.

Huang, Beijia, et al. “A Life Cycle Thinking Framework to Mitigate the Environmental Impact of Building Materials.” One Earth, vol. 3, no. 5, Nov. 2020, pp. 564–73. ScienceDirect, https://doi.org/10.1016/j.oneear.2020.10.010.

IPCC, 2014: Climate Change 2014: Synthesis Report. Contribution of Working Groups I, II and III to the Fifth Assessment Report of the Intergovernmental Panel on Climate Change [Core Writing Team, R.K. Pachauri and L.A. Meyer (eds.)]. IPCC, Geneva, Switzerland, 151 pp.

Jacques, D., et al. “Modelling Chemical Degradation of Concrete during Leaching with Rain and Soil Water Types.” Cement & Concrete Research, vol. 40, no. 8, Aug. 2010, pp. 1306–13. a9h.

Janssen, B. H. “Nitrogen Mineralization in Relation to C:N Ratio and Decomposability of Organic Materials.” Progress in Nitrogen Cycling Studies: Proceedings of the 8th Nitrogen Workshop Held at the University of Ghent, 5–8 September, 1994, edited by O. Van Cleemput et al., Springer Netherlands, 1996, pp. 69–75. Springer Link, https://doi.org/10.1007/978-94-011-5450-5_13.

Jiang, Yi, et al. “Characteristics of Steel Slags and Their Use in Cement and Concrete—A Review.” Resources, Conservation, and Recycling, vol. 136, Jan. 2018, pp. 187–97. agr, EBSCOhost, https://doi.org/10.1016/j.resconrec.2018.04.023.

Jorat, M. Ehsan, et al. “Passive CO2 Removal in Urban Soils: Evidence from Brownfield Sites.” Science of The Total Environment, vol. 703, Feb. 2020, p. 135573. DOI.org (Crossref), https://doi.org/10.1016/j.scitotenv.2019.135573.

Kamal, Nur Liyana Mohd, et al. “Carbon Dioxide Sequestration in Concrete and Its Effects on Concrete Compressive Strength.” Materials Today: Proceedings, vol. 31, 2020, pp. A18–21. DOI.org (Crossref), https://doi.org/10.1016/j.matpr.2020.11.185.

Kantzas, Euripides P., et al. “Substantial Carbon Drawdown Potential from Enhanced Rock Weathering in the United Kingdom.” Nature Geoscience, vol. 15, no. 5, 5, May 2022, pp. 382–89. www-nature-com.proxy.lib.ohio-state.edu, https://doi.org/10.1038/s41561-022-00925-2.

Kaushal, Sujay S., Julia Gorman, et al. “Human-Accelerated Weathering Increases Salinization, Major Ions, and Alkalinization in Fresh Water across Land Use.” Applied Geochemistry, vol. 83, Jan. 2017, pp. 121–35. agr, EBSCOhost, https://doi.org/10.1016/j.apgeochem.2017.02.006.

Kelemen, Peter B., et al. “Rates and Mechanisms of Mineral Carbonation in Peridotite: Natural Processes and Recipes for Enhanced, in Situ CO 2 Capture and Storage.” Annual Review of Earth and Planetary Sciences, vol. 39, no. 1, May 2011, pp. 545–76. DOI.org (Crossref), https://doi.org/10.1146/annurev-earth-092010-152509.

Kharbush, Jenan J., et al. “Patterns in Sources and Forms of Nitrogen in a Large Eutrophic Lake during a Cyanobacterial Harmful Algal Bloom.” Limnology and Oceanography, vol. n/a, no. n/a, Feb. 2023. Wiley Online Library, https://doi.org/10.1002/lno.12311.

Knobeloch, L., et al. “Blue Babies and Nitrate-Contaminated Well Water.” Environmental Health Perspectives, vol. 108, no. 7, July 2000, pp. 675–78. ehp.niehs.nih.gov (Atypon), https://doi.org/10.1289/ehp.00108675.

Lackner, Klaus S. “Carbonate Chemistry for Sequestering Fossil Carbon.” Annual Review of Energy and the Environment, vol. 27, no. 1, Nov. 2002, pp. 193–232. DOI.org (Crossref), https://doi.org/10.1146/annurev.energy.27.122001.083433.

Langer, William H., et al. “Accelerated Weathering of Limestone for CO2 Mitigation: Opportunities for the Stone and Cement Industries.” Mining Engineering, vol. 61, no. 2, Mar. 2009, pp. 27–32. asf.

Lee, Han-seung, and Xiao-Yong Wang. Evaluation of the Carbon Dioxide Uptake of Slag-Blended Concrete Structures, Considering the Effect of Carbonation. 2016. Semantic Scholar, https://doi.org/10.3390/SU8040312.

Mamlouk, Michael S., and John P. Zaniewski. Materials for Civil and Construction Engineers. Fourth edition, Pearson Education, Inc, 2016.

Manning, David A. C., and Phil Renforth. “Passive Sequestration of Atmospheric CO2 through Coupled Plant-Mineral Reactions in Urban Soils.” Environmental Science & Technology, vol. 47, no. 1, Jan. 2013, pp. 135–41. ACS Publications, https://doi.org/10.1021/es301250j.

Manning, D. A. C., et al. “Carbonate Precipitation in Artificial Soils Produced from Basaltic Quarry Fines and Composts: An Opportunity for Passive Carbon Sequestration.” International Journal of Greenhouse Gas Control, vol. 17, Sept. 2013, pp. 309–17. ScienceDirect, https://doi.org/10.1016/j.ijggc.2013.05.012.

Miller, R.O., R. Gavlak, and D. Horneck. 2013. Saturated paste extract for calcium, magnesium, sodium and SAR. p. 21-22. In Soil, plant and water methods for the western region. WREP-125. 4th ed.

Mindess, Sidney, et al. Concrete. 2nd ed., Prentice Hall, 2003.

Moore, Joel, et al. “Concrete Weathering and the Urban Built Environment as a Major Source of Increased Major Ion Concentrations Including Dissolved Inorganic Carbon and Weathering Fluxes in Urban Watersheds.” Abstracts with Programs - Geological Society of America, vol. 49, no. 2, 2017, p. @Abstract no. 65-3. geh.

National Academy of Sciences. 2020. Climate Change: Evidence and Causes: Update 2020. Washington, DC: The National Academies Press. https://doi.org/10.17226/25733.

Ngala, V. T., and C. L. Page. “EFFECTS OF CARBONATION ON PORE STRUCTURE AND DIFFUSIONAL PROPERTIES OF HYDRATED CEMENT PASTES.” Cement and Concrete Research, vol. 27, no. 7, July 1997, pp. 995–1007. DOI.org (Crossref), https://doi.org/10.1016/S0008-8846(97)00102-6.

Oates, Tony. “Lime and Limestone.” Kirk-Othmer Encyclopedia of Chemical Technology, John Wiley & Sons, Ltd, 2010, pp. 1–53. Wiley Online Library, https://doi.org/10.1002/0471238961.1209130507212019.a01.pub3.

ODNR, Division of Soil and Water. Precipitation in Ohio. Fact Sheet 92-11, 7 Oct. 2011.

Ortega-López, Vanesa, et al. “Durability Studies on Fiber-Reinforced EAF Slag Concrete for Pavements.” Construction & Building Materials, vol. 163, Feb. 2018, pp. 471–81. a9h.

Oskierski, Hans C., et al. “Sequestration of Atmospheric CO (Sub 2) in Chrysotile Mine Tailings of the Woodsreef Asbestos Mine, Australia; Quantitative Mineralogy, Isotopic Fingerprinting and Carbonation Rates.” Chemical Geology, vol. 358, Nov. 2013, pp. 156–69. geh, EBSCOhost, https://doi.org/10.1016/j.chemgeo.2013.09.001.

Panesar, Daman K. “Supplementary Cementing Materials.” Developments in the Formulation and Reinforcement of Concrete, Elsevier, 2019, pp. 55–85. DOI.org (Crossref), https://doi.org/10.1016/B978-0-08-102616-8.00003-4.

Possan, Edna, et al. “CO2 Uptake Potential Due to Concrete Carbonation: A Case Study.” Case Studies in Construction Materials, vol. 6, June 2017, pp. 147–61. ScienceDirect, https://doi.org/10.1016/j.cscm.2017.01.007.

Rabalais, Nancy N., and R. Eugene Turner. “Gulf of Mexico Hypoxia: Past, Present, and Future.” Limnology and Oceanography Bulletin, vol. 28, no. 4, 2019, pp. 117–24. Wiley Online Library, https://doi.org/10.1002/lob.10351.

Ravikumar, Dwarakanath, et al. “Carbon Dioxide Utilization in Concrete Curing or Mixing Might Not Produce a Net Climate Benefit.” Nature Communications, vol. 12, no. 1, Dec. 2021, p. 855. DOI.org (Crossref), https://doi.org/10.1038/s41467-021-21148-w.

Renforth, Phil. “The Potential of Enhanced Weathering in the UK.” International Journal of Greenhouse Gas Control, vol. 10, Sept. 2012, pp. 229–43. ScienceDirect, https://doi.org/10.1016/j.ijggc.2012.06.011.

Renforth, Phil. “The Negative Emission Potential of Alkaline Materials.” Nature Communications, vol. 10, no. 1, 1, Mar. 2019, p. 1401. www.nature.com, https://doi.org/10.1038/s41467-019-09475-5.

Renforth, Phil, and David A. C. Manning. “Laboratory Carbonation of Artificial Silicate Gels Enhanced by Citrate: Implications for Engineered Pedogenic Carbonate Formation.” International Journal of Greenhouse Gas Control, vol. 5, no. 6, Nov. 2011, pp. 1578–86. 8gh.

Renforth, Phil., C. L. Washbourne, et al. “Silicate Production and Availability for Mineral Carbonation.” Environmental Science & Technology, vol. 45, no. 6, Mar. 2011, pp. 2035–41. asf.

Renforth, Phil, et al. “Carbonate Precipitation in Artificial Soils as a Sink for Atmospheric Carbon Dioxide.” Applied Geochemistry, vol. 24, no. 9, Sept. 2009, pp. 1757–64. Heriot-Watt Research Portal, https://doi.org/10.1016/j.apgeochem.2009.05.005.

Renforth, Phil., et al. “The Dissolution of Olivine Added to Soil: Implications for Enhanced Weathering.” Applied Geochemistry, vol. 61, Oct. 2015, pp. 109–18. DOI.org (Crossref), https://doi.org/10.1016/j.apgeochem.2015.05.016.

Rousk, Johannes, et al. “Contrasting Soil PH Effects on Fungal and Bacterial Growth Suggest Functional Redundancy in Carbon Mineralization.” Applied and Environmental Microbiology, vol. 75, no. 6, Mar. 2009, pp. 1589–96. PubMed Central, https://doi.org/10.1128/AEM.02775-08.

Ruschi Mendes Saade, Marcella, et al. “Is Crushed Concrete Carbonation Significant Enough to Be Considered as a Carbon Mitigation Strategy?” Environmental Research Letters, vol. 17, no. 10, Oct. 2022, p. 104049. DOI.org (Crossref), https://doi.org/10.1088/1748-9326/ac9490.

Saleh, Hosam M., and Samir B. Eskander. “18 - Innovative Cement-Based Materials for Environmental Protection and Restoration.” New Materials in Civil Engineering, edited by Pijush Samui et al., Butterworth-Heinemann, 2020, pp. 613–41. ScienceDirect, https://doi.org/10.1016/B978-0-12-818961-0.00018-1.

Schlesinger, William H. “Carbon storage in the Caliche of arid soils: A case study from Arizona.” Soil Science, vol. 133, no. 4, Apr. 1982, p. 247.

Schuiling, R. D. “Carbon Dioxide Sequestration, Weathering Approaches To.” Geoengineering Responses to Climate Change: Selected Entries from the Encyclopedia of Sustainability Science and Technology, edited by Tim Lenton and Naomi Vaughan, Springer, 2013, pp. 141–67. Springer Link, https://doi.org/10.1007/978-1-4614-5770-1_7.

Schuiling, R.D., Krijgsman, P. Enhanced Weathering: An Effective and Cheap Tool to Sequester Co2 . Climatic Change 74, 349–354 (2006). https://doi.org/10.1007/s10584-005-3485-y

Schutter, Mary E., and Richard P. Dick. "c." Soil Science Society of America Journal, vol. 64, no. 5, Sept. 2000, pp. 1659–68. DOI.org (Crossref), https://doi.org/10.2136/sssaj2000.6451659x.

Shao, Yixin, et al. "CO2 Sequestration Using Calcium-Silicate Concrete." Canadian Journal of Civil Engineering, vol. 33, no. 6, June 2006, pp. 776–84. cdnsciencepub.com (Atypon), https://doi.org/10.1139/l05-105.

Shao, Yixin, and Xiaolu Lin. "Early-Age Carbonation Curing of Concrete Using Recovered CO2." Concrete International, vol. 33, no. 9, Sept. 2011, pp. 50–56. asf.

Sheldrick, B. H. and C Wang. 1993. Particle-size Distribution. pp. 499-511. In: Carter, M. R. (ed), Soil Sampling and Methods of Analysis, Canadian Society of Soil Science, Lewis Publishers, Ann Arbor, MI.

Stehouwer, Richard C., et al. "Acidic Soil Amendment with a Magnesium-Containing Fluidized Bed Combustion By-Product." Agronomy Journal, vol. 91, no. 1, 1999, pp. 24–32. Wiley Online Library, https://doi.org/10.2134/agronj1999.00021962009100010005x.

Stehouwer, R. C., et al. "Use of Clean Coal Technology By-Products as Agricultural Liming Techniques." 11. International Symposium on Use and Management of Coal Combustion by-Products (CCBs), Orlando, FL (United States), 15-19 Jan 1995, DOE/MC/28060--95/C0445, Dravo Lime Co., Pittsburgh, PA (United States), Mar. 1995, https://digital.library.unt.edu/ark:/67531/metadc675521/.

Takano, Hiroyuki, and Tadashi Matsunaga. "CO2 Fixation by Artificial Weathering of Waste Concrete and Coccolithophorid Algae Cultures." Energy Conversion & Management, vol. 36, no. 6–9, Sept. 1995, p. 697. iih.

Taylor, Lyla L., et al. "Enhanced Weathering Strategies for Stabilizing Climate and Averting Ocean Acidification." Nature Climate Change, vol. 6, no. 4, Apr. 2016, pp. 402–06. DOI.org (Crossref), https://doi.org/10.1038/nclimate2882.

ten Berge, Hein F. M., et al. "Olivine Weathering in Soil, and Its Effects on Growth and Nutrient Uptake in Ryegrass (Lolium Perenne L.): A Pot Experiment." PLOS ONE, vol. 7, no. 8, Aug. 2012, p. e42098, https://doi.org/10.1371/journal.pone.0042098.

Thornbush, Mary J., and H. A. Viles. “Simulation of the Dissolution of Weathered versus Unweathered Limestone in Carbonic Acid Solutions of Varying Strength.” Earth Surface Processes and Landforms, vol. 32, no. 6, May 2007, pp. 841–52. geh, EBSCOhost, https://doi.org/10.1002/esp.1441.

Torres-Carrasco, M., et al. “New Insights in Weathering Analysis of Anhydrous Cements by Using High Spectral and Spatial Resolution Confocal Raman Microscopy.” Cement & Concrete Research, vol. 100, Oct. 2017, pp. 119–28. a9h.

US EPA. Estimated Nitrate Concentrations in Groundwater Used for Drinking. 11 Jan. 2023, https://www.epa.gov/nutrient-policy-data/estimated-nitrate-concentrations-groundwater-used-drinking.

US EPA. What Is Acid Rain? 9 Feb. 2016, https://www.epa.gov/acidrain/what-acid-rain.

U.S. Geological Survey, 2022, Mineral commodity summaries 2022: U.S. Geological Survey, 202 p., https://doi.org/10.3133/mcs2022.

Vanderzee, Sterling, and Frank Zeman. “Recovery and Carbonation of 100% of Calcium in Waste Concrete Fines: Experimental Results.” Journal of Cleaner Production, vol. 174, Feb. 2018, pp. 718–27. ScienceDirect, https://doi.org/10.1016/j.jclepro.2017.10.257.

Washbourne, C.-L., et al. “Investigating Carbonate Formation in Urban Soils as a Method for Capture and Storage of Atmospheric Carbon.” Science of the Total Environment, vol. 431, Jan. 2012, pp. 166–75. agr, EBSCOhost, https://doi.org/10.1016/j.scitotenv.2012.05.037.

Washbourne, Carla-Leanne, et al. “Rapid Removal of Atmospheric CO2 by Urban Soils.” Environmental Science & Technology, vol. 49, no. 9, Jan. 2015, pp. 5434–40. agr.

Williamson, Phil. “Emissions Reduction: Scrutinize CO2 Removal Methods.” Nature, vol. 530, no. 7589, 7589, Feb. 2016, pp. 153–55. www-nature-com.proxy.lib.ohio-state.edu, https://doi.org/10.1038/530153a.

Xi, F., Davis, S., Ciais, P. et al. Substantial global carbon uptake by cement carbonation. Nature Geosci 9, 880–883 (2016). https://doi.org/10.1038/ngeo2840

Yang, Keun-Hyeok, et al. “Carbonation and CO2 Uptake of Concrete.” Environmental Impact Assessment Review, vol. 46, Apr. 2014, pp. 43–52. ScienceDirect, https://doi.org/10.1016/j.eiar.2014.01.004.

Yoder, R.E. 1936. A direct method of aggregate of analysis and a study of the physical nature of erosion losses. J. Am. Soc. Agron. 28:337-351.

Zamanian, Kazem, et al. “Pedogenic Carbonates: Forms and Formation Processes.” Earth-Science Reviews, vol. 157, June 2016, pp. 1–17. ScienceDirect, https://doi.org/10.1016/j.earscirev.2016.03.003.

Zhang, Duo, and Yixin Shao. “Effect of Early Carbonation Curing on Chloride Penetration and Weathering Carbonation in Concrete.” Construction & Building Materials, vol. 123, Oct. 2016, pp. 516–26. a9h.

Appendix A. Modeling Calculations

sample	conc	calcium_mol	sulfate_mol	silica_mol	co2_mol	co2_g	ett_mol	csh_mol	co2_g_ett	co2_g_csh	co2_total_g
C	1000	0.00078	0.00011	0.00008	0.00113	0.04966	0.00011	0.00023	0.00835	0.00424	0.05595
C	1000	0.00065	0.00009	0.00006	0.00091	0.04005	0.00009	0.00017	0.00648	0.00314	0.04486
C	1000	0.00057	0.00019	0.00016	0.00123	0.05412	0.00019	0.00047	0.01389	0.00869	0.06541
C	1000	0.00092	0.00017	0.00014	0.00151	0.06639	0.00017	0.00041	0.01279	0.00754	0.07655
L	119	0.00245	0.00041	0.00101	0.00589	0.25908	0.00041	0.00302	0.03040	0.05541	0.30198
L	120	0.00160	0.00036	0.00056	0.00363	0.15966	0.00036	0.00167	0.02645	0.03053	0.18815
L	116	0.00000	0.00016	0.00008	0.00040	0.01778	0.00016	0.00025	0.01156	0.00451	0.02582
L	123	0.00096	0.00022	0.00034	0.00219	0.09648	0.00022	0.00101	0.01608	0.01851	0.11377
F	148	0.01563	0.01232	0.00124	0.03167	1.39376	0.01232	0.00373	0.90287	0.06834	1.87936
F	147	0.01696	0.01111	0.00190	0.03376	1.48559	0.01111	0.00569	0.81458	0.10426	1.94502
F	146	0.01198	0.00937	0.00134	0.02537	1.11646	0.00937	0.00402	0.68682	0.07371	1.49673
F	135	0.01544	0.01316	0.00101	0.03162	1.39178	0.01316	0.00303	0.96463	0.05555	1.90187
MODEL	1000	0.08543	0.04115	0.00282	0.13503	5.94270	0.04115	0.00845	3.01678	0.15496	7.52857
MODEL	750	0.07286	0.04065	0.00293	0.12230	5.38262	0.04065	0.00879	2.98026	0.16119	6.95335
MODEL	500	0.04986	0.02908	0.00320	0.08853	3.89604	0.02908	0.00959	2.13170	0.17575	5.04977
MODEL	130	0.01483	0.00931	0.00440	0.03733	1.64271	0.00931	0.01319	0.68290	0.24166	2.10499
MODEL	50	0.00687	0.00398	0.00559	0.02761	1.21499	0.00398	0.01676	0.29182	0.30716	1.51448

Appendix B. Air Sample Data

Methane Concentration (ppm)

	sample							
	1	2	3	4	5	6	7	8
sampled	7/12/2022	7/26/2022	8/9/2022	8/23/2022	9/6/2022	9/20/2022	10/4/2022	10/18/2022
analyzed	7/19/2022	7/28/2022	8/15/2022	8/24/2022	9/6/2022	x	x	x
C1	4.749	4.06	2.48	3.791	2.325	1.928	3.23	3.464
C2	4.979	4.023	2.488	3.452	2.26	1.851	3.208	3.332
C3	5.292	3.408	2.524	3.582	2.322	1.993	3.1	3.203
C4	4.799	3.485	2.836	3.521	2.374	1.915	3.155	3.489
L1	4.187	3.041	2.32	2.625	2.011	1.589	2.702	2.75
L2	4.537	3.199	2.349	3.121	2.109	1.651	2.54	3.305
L3	4.506	3.059	2.312	3.192	2.008	2.019	3.098	3.202
L4	4.561	3.168	2.352	2.723	2.001	1.704	2.88	3.426
F1	5.012	3.54	2.606	3.089	2.227	1.693	2.514	2.87
F2	4.905	3.279	2.341	3.455	2.321	1.85	2.822	3.35
F3	5.381	3.226	2.437	3.27	2.173	1.749	3.237	3.387
F4	5.94	36.079	3.427	3.33	2.187	1.381	2.362	3.017
S1	4.876	3.281	2.341	3.715	1.983	1.926	2.469	7.937
S2	4.57	3.106	2.371	3.1	2.044	1.689	2.298	2.112
S3	5.217	3.457	2.228	5.435	2.251	1.897	4.217	3.335
S4	4.698	3.649	2.281	3.299	2.2	1.998	1.949	3.588

Carbon Dioxide Concentration (ppm)

	sample							
	1	2	3	4	5	6	7	8
sampled	7/12/2022	7/26/2022	8/9/2022	8/23/2022	9/6/2022	9/20/2022	10/4/2022	10/18/2022
analyzed	7/19/2022	7/28/2022	8/15/2022	8/24/2022	13-Sep	x	x	x
C1	145.091	280.191	338.15	148.772	398.878	397.634	339.446	327.035
C2	140.068	100.726	287.564	137.938	376.845	393.151	281.918	281.158
C3	112.804	149.679	284.245	167.06	437.997	460.119	321.949	286.794
C4	190.386	163.869	306.469	218.053	437.769	422.308	387.296	386.803
L1	1632.618	3325.704	383.931	8879.352	425.227	423.928	838.863	966.74
L2	909.492	1338.343	334.03	1320.472	435.225	469.257	3001.101	3361.022
L3	787.601	1289.725	349.841	880.573	418.248	450.224	810.197	788.458
L4	1461.449	3454.615	324.859	3965.609	529.715	500.247	1248.859	1272.86
F1	96.784	58.886	299.282	267.75	373.663	441.015	3352.452	3942.685
F2	188.885	382.81	335.643	919.011	472.837	412.039	1590.246	1394.239
F3	172.254	306.821	323.561	361.443	395.682	445.543	784.994	752.823
F4	290.812	447.633	347.516	1199.919	438.475	406.174	4297.019	3414.192
S1	1558.92	3191.718	338.385	4645.155	513.9	454.55	4999.135	4426.749
S2	1020.702	1102.824	325.499	1410.927	435.466	541.543	6892.401	487.999
S3	909.01	3125.554	381.368	6557.218	582.955	533.036	8622.137	7989.019
S4	800.914	3785.656	366.697	1885.669	404.527	664.629	475.204	6437.937

Nitrous Oxide Concentration (ppm)

		sample		
		6	7	8
sampled		9/20/2022	10/4/2022	10/18/2022
analyzed	x	x	x	
C1		0.459	0.479	0.501
C2		0.478	0.471	0.491
C3		0.454	0.483	0.471
C4		0.455	0.491	0.484
L1		0.473	0.529	0.508
L2		0.484	0.588	0.578
L3		0.462	0.541	0.56
L4		0.483	0.788	0.662
F1		0.466	1.038	2.168
F2		0.467	0.725	0.755
F3		0.479	0.481	0.534
F4		0.48	0.707	0.705
S1		0.482	0.823	0.603
S2		0.614	5.602	0.508
S3		0.538	1.463	1.121
S4		0.491	0.499	0.474